Development 140, 1665-1675 (2013) doi:10.1242/dev.087387

Tcf7l1 prepares epiblast cells in the gastrulating mouse embryo for lineage specification

Jackson A. Hoffman, Chun-I Wu and Bradley J. Merrill*

SUMMARY

The core gene regulatory network (GRN) in embryonic stem cells (ESCs) integrates activities of the pro-self-renewal factors Oct4 (Pou5f1), Sox2 and Nanog with that of an inhibitor of self-renewal, Tcf7l1 (Tcf3). The inhibitor function of Tcf7l1 causes dependence on extracellular Wnt/β-catenin signaling activity, making its embryonic role within the ESC GRN unclear. By analyzing intact mouse embryos, we demonstrate that the function of Tcf7l1 is necessary for specification of cell lineages to occur concomitantly with the elaboration of a three-dimensional body plan during gastrulation. In *Tcf7l1*$^{-/-}$ embryos, specification of mesoderm is delayed, effectively uncoupling it from the induction of the primitive streak. Tcf7l1 repressor activity is necessary for a rapid switch in the response of pluripotent cells to Wnt/β-catenin stimulation, from one of self-renewal to a mesoderm specification response. These results identify Tcf7l1 as a unique factor that is necessary in pluripotent cells to prepare them for lineage specification. We suggest that the role of Tcf7l1 in mammals is to inhibit the GRN to ensure the coordination of lineage specification with the dynamic cellular events occurring during gastrulation.

KEY WORDS: EpiSC, Primitive streak, Tcf3, Tcf7l1, Wnt

INTRODUCTION

Mammals are unlike most other animals in that the small zygote requires substantial cell proliferation before the elaboration of a basic body plan can begin. During the growth of the early embryo, individual cells must retain the ability to make all adult cell types, i.e. pluripotency. Understanding mechanisms that control pluripotency is an important goal of stem cell research and was stimulated by the discovery of conditions enabling embryonic stem cell (ESC) cultures to be derived from outgrowths of the blastocyst inner cell mass (ICM) (Evans and Kaufman, 1981; Martin, 1981).

In vitro experiments with ESCs showed that the Oct4 (Pou5f1 – Mouse Genome Informatics), Sox2 and Nanog transcription factors constitute core components of a gene regulatory network (GRN) that stimulates self-renewal of pluripotent cells. The GRN model is supported by overlapping sites of chromatin occupancy for Oct4, Sox2 and Nanog proteins, including on one another's genes (Boyer et al., 2005; Cole et al., 2008; Loh et al., 2006; Marson et al., 2008), and extensive protein-protein interactions between the three factors (Chambers and Tomlinson, 2009; Kim et al., 2008; Liang et al., 2008; Wang et al., 2006). Tcf7l1 (formerly Tcf3) has been identified as a crucial regulator of the pluripotency GRN in ESCs by studies showing that Tcf7l1 co-occupies Oct4, Sox2 and Nanog sites in chromatin (Cole et al., 2008; Marson et al., 2008; Tam et al., 2008) and that Tcf7l1 regulates the expression of Oct4 and Nanog target genes (Cole et al., 2008; Pereira et al., 2006; Tam et al., 2008; Yi et al., 2008). Recently, the Esrrb transcription factor was identified as a direct target of Tcf7l1 regulation important for Tcf7l1-mediated effects on self-renewal *in vitro* (Martello et al., 2012).

Whereas Esrrb, Oct4, Sox2 and Nanog all stimulate self-renewal, genetic experiments unequivocally show that Tcf7l1 inhibits self-renewal (Guo et al., 2011; Pereira et al., 2006; Salomonis et al., 2010; Wray et al., 2011; Yi et al., 2011; Yi et al., 2008). Interestingly, Tcf7l1 is a transcriptional repressor in the Wnt/β-catenin pathway (Wu et al., 2012), and Wnt activity is necessary for mouse ESC self-renewal (ten Berge et al., 2011). Ablating Tcf7l1 is sufficient to replace a requirement for Wnt/β-catenin signaling, indicating that endogenous Tcf7l1 expression causes ESC dependence on Wnt/β-catenin (Wray et al., 2011; Yi et al., 2011). Conversely, Wnt3a treatment rescues self-renewal in ESCs inhibited by Tcf7l1 overexpression (Yi et al., 2011). Roles for Tcf7l1 in differentiation have been suggested, but *in vitro* differentiation assays have revealed only minor and variable lineage specification defects in Tcf7l1-deficient ESCs (Pereira et al., 2006; Salomonis et al., 2010; Tam et al., 2008). Thus, whereas the embryonic function of factors that stimulate the GRN (i.e. Oct4, Nanog and Sox2) is clearly necessary to stimulate the self-renewal of pluripotent cells as early embryos expand (Avilion et al., 2003; Mitsui et al., 2003; Nichols et al., 1998), an embryonic function for an inhibitor of GRN activity, such as Tcf7l1, has not been elucidated. As such, it is not clear why pluripotent cells express high levels of an ostensible inhibitor of their self-renewal.

With a perspective that the evolution of the pluripotency GRN in mammals included the Tcf7l1 inhibitor activity to enable some aspect of early embryogenesis, we reasoned that examining embryogenesis in *Tcf7l1* mutant embryos would elucidate a role for Tcf7l1 in pluripotent cells. Building upon previous work showing that Oct4, Sox2, Nanog and Tcf7l1 are expressed during gastrulation (Avilion et al., 2003; Hart et al., 2004; Merrill et al., 2004; Morkel et al., 2003; Yamaguchi et al., 2005; Yeom et al., 1996), we define changes in their protein expression that occur in epiblast cells prior to and during cell lineage specification. Gene expression defects in *Tcf7l1*$^{-/-}$ embryos coincided with a delay in the specification of mesoderm at the primitive streak region, demonstrating that Tcf7l1 is necessary to couple lineage specification with primitive streak morphogenesis. *In vitro*, ESCs required Tcf7l1 to rapidly convert to a state in which they formed mesoderm in response to Wnt/β-catenin signaling. We suggest that the activity of Tcf7l1 as a negative regulator of the pluripotency GRN is closely related to its

Department of Biochemistry and Molecular Genetics, University of Illinois at Chicago, Chicago, IL 60607, USA.

*Author for correspondence (merrillb@uic.edu)

Accepted 7 February 2013

first embryonic function, which enables appropriate responses to lineage specification signals.

MATERIALS AND METHODS

Preparation of embryos for multi-dimensional expression analysis

Embryos were fixed within decidua for 1 hour at 4°C in 4% paraformaldehyde (PFA), washed in PBS, and cryopreserved by washing in 15% sucrose for 1 hour at room temperature and in 30% sucrose overnight at 4°C. Transverse 8 μm sections through entire embryos were taken using a Microm HM550 cryostat and collected four to a slide in groups of four slides at a time, such that the first slide contained sections #1, #5, #9 and #13, the second slide sections #2, #6, #10 and #14, and so on. This enabled tracking of the position of sections along the proximal-distal axis of each embryo, orientation of the anterior-posterior axis, and use of adjacent epiblast sections for four individual experiments. For each assay, sections throughout the entire proximal-distal axis of each embryo were used. Embryos were staged by morphological features (Downs and Davies, 1993) and expression of brachyury, an early marker of mesoderm cells at the primitive streak (PS) (supplementary material Fig. S1A) (Wilkinson et al., 1990). Unless multiple sections of single embryos are depicted, as in Fig. 4, the images show embryo sections from the proximal epiblast, as depicted in supplementary material Fig. S1A.

Immunofluorescent staining

Embryo sections for immunofluorescence staining were fixed for 8-10 minutes in cold 4% PFA, washed with PBS, blocked for 1 hour at room temperature in 1% BSA, 0.1% Triton X-100 and 5% normal donkey serum, and treated overnight at 4°C with the following antibodies diluted in blocking solution: rabbit anti-Tcf7l1 (Pereira et al., 2006) (1:500), rat anti-E-cadherin (1:100, M. Takeichi, DHSB), rabbit anti-Nanog (1:100, Abcam), goat anti-Oct4 (1:500, Santa Cruz), goat anti-Sox2 (1:500, Santa Cruz) and goat anti-brachyury (1:500, Santa Cruz). FITC-, Texas Red- and Cy5-conjugated secondary antibodies (Jackson ImmunoResearch) were used at 1:100. Immunofluorescence was imaged using a Zeiss LSM 700 or Zeiss LSM 5 Pascal microscope.

Quantification was performed on proximal epiblast sections of early-streak embryos. Individual detection channels were separately imported into Photoshop (Adobe) as individual RGB channels to create composite images in which each channel could be analyzed separately or together. The center of the PS in each embryo was identified by cell morphology and the presence of Prickle1 expression in nearby sections from the same embryo. Each nucleus was numbered and its distance from the center of the PS was calculated using the Ruler and Measurement tool. The Quick Selection tool outlined each nucleus and the Measurement tool determined mean signal intensity. Distance measurements were normalized to the entire length of the epiblast, and expression of each protein was normalized to the mean level of protein expression in each embryo. Four $Tcf7l1^{+/+}$ and $Tcf7l1^{-/-}$ embryos and two Nanog-overexpressing embryos were examined for quantification of each protein. Pearson correlation coefficients (r) were calculated in Microsoft Excel 2007. The statistical significance of the Pearson correlation was determined using a two-tailed Student's t-test in Excel.

In situ hybridization

Whole-mount *in situ* hybridization was performed as described (Merrill et al., 2004). Probes for brachyury, *Nanog*, *Gsc* and *Prickle1* were kind gifts from D. Wilkinson (Wilkinson et al., 1990), I. Chambers (Chambers et al., 2003), E. DeRobertis (Conlon et al., 1994) and T. Rodriguez (Crompton et al., 2007), respectively. All other probes were PCR cloned from cDNA or genomic DNA corresponding to the following regions of the full-length Ensembl cDNA sequence: *Mixl1* (bp 994-2175), *Oct4* (bp 469-935) and *Sox1* (bp 2325-2681).

ESC transition assays

Mouse ESCs were maintained on gelatin-coated plates in serum-containing medium [Knockout DMEM (Gibco) supplemented with 15% fetal calf serum (Atlanta Biologicals)]. The ESC transition procedure was adapted from previous work (Guo et al., 2009). Briefly, ESCs were plated at 2×10^4 cells/cm^2 in serum-containing ESC media on fibronectin (Millipore)-coated plates. After 24 hours, media were replaced with N2B27 media (Gibco) containing 20 ng/ml activin A (R&D Systems) and 12 ng/ml Fgf2 (R&D Systems). Cells were given fresh medium every day, and were passaged with Dispase (Roche) every 2 days. CHIR99021 (Stemgent) was added to N2B27 media to a final concentration of 3 μM at 24-hour time points as depicted in Fig. 6A. For ESC colony formation assays, colonies were trypsinized to a single-cell suspension and plated in normal ESC culture conditions at 1000 cells per well, and scored for ESC-like colonies after 4 days

Generation of doxycycline-inducible *Nanog* transgenic mice and *in vivo* induction of Nanog expression

Standard molecular biology techniques were used to construct a targeting vector. Briefly, *Nanog* cDNA was cloned from pPyCagNanogIP (a kind gift of Dr Ian Chambers) into a vector containing a Tet operator (TetO) and upstream and downstream polyadenylation sequences (Chambers et al., 2003). This TetO-Nanog cassette was then cloned into an HPRT targeting vector and electroporated into F3 ESCs (both kind gifts of Dr Stephen Duncan) (Misra et al., 2001). Four independent ESC clones were injected by the UIC Core Transgenic Facility into recipient C57BL/6 blastocysts for germline transmission. Males harboring this TetO-Nanog gene cassette were mated to females ubiquitously expressing the reverse tetracycline transactivator from the *Rosa26* locus (derived from JAX stock #005670) and females were checked for vaginal plugs daily. Pregnant females were fed chow containing 200 mg/kg doxycycline (Bioserv) at embryonic day (E) 2.5 to induce Nanog expression throughout the epiblast prior to the pre-streak stage (supplementary material Fig. S4E). Owing to the integration of the TetO-Nanog cassette into the *Hprt* locus on the X-chromosome and X-inactivation of the paternal X-chromosome in extra-embryonic tissues, this mating scheme restricted Nanog overexpression to the epiblast.

RESULTS

Dynamic expression of pluripotency factors during gastrulation

Previous studies showed that pluripotency factors (Tcf7l1, Oct4, Sox2 and Nanog) are expressed in the epiblast at the time of lineage specification (Avilion et al., 2003; Hart et al., 2004; Merrill et al., 2004; Morkel et al., 2003; Yamaguchi et al., 2005; Yeom et al., 1996). Each of these analyses focused on a single factor or provided limited data for multiple stages of gastrulation. Comparisons of factor expression were further obscured by the combination of the speed of progression through gastrulation (Downs and Davies, 1993; Rivera-Pérez et al., 2010), differences in embryo staging, and different types of expression analyses among the studies. In addition, cell-based experiments demonstrated that relatively small changes in the levels of Oct4, Sox2 and Nanog have a significant influence on the specification of lineages during differentiation *in vitro* (Chambers et al., 2003; Mitsui et al., 2003; Niwa et al., 2000; Thomson et al., 2011). Thus, although the previous reports combine to demonstrate the expression of pluripotency factors during gastrulation, analysis of expression was not completed with sufficient precision to compare the relative levels of factors.

We used two complementary methods to examine pluripotency factor expression during gastrulation. First, changes in the patterns of expression were determined during progression through the pre-streak, early-streak and mid-streak stages of gastrulation. Brachyury protein was absent from pre-streak embryos (Fig. 1A), but appeared in early-streak embryos, where it marked the posterior epiblast prior to formation of a nascent layer of mesoderm (Fig. 1A′), which was evident later in mid-streak embryos (Fig. 1A″). Tcf7l1 was uniformly expressed throughout the epiblast of pre-streak embryos, but began to reduce near the primitive streak (PS) of early-streak embryos, and progressively diminished in the posterior epiblast through gastrulation (Fig. 1B-B″). Oct4 protein expression remained uniform throughout the epiblast of pre-, early- and mid-streak

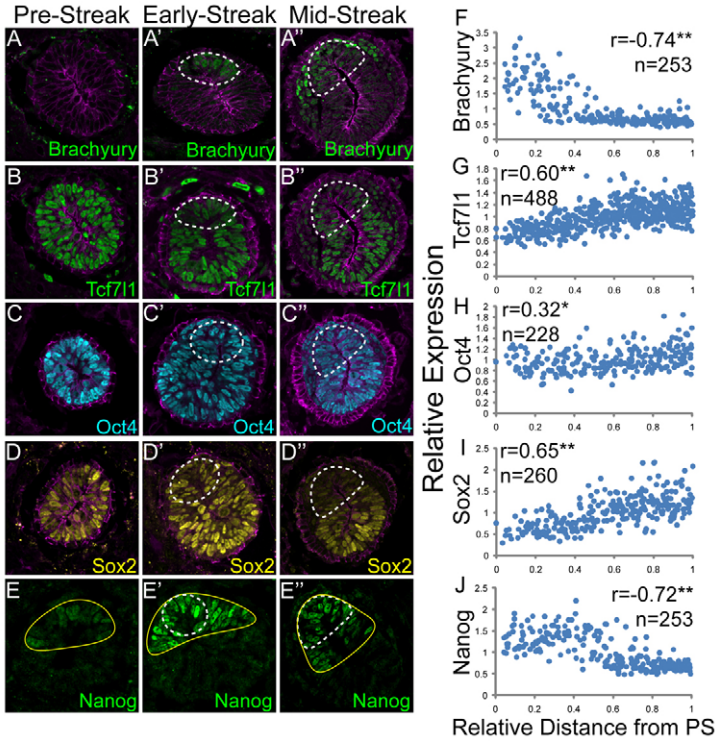

Fig. 1. Dynamic expression of pluripotency gene regulatory network components during gastrulation.
(**A-E″**) Immunofluorescent staining from a representative transverse cryosection of a wild-type mouse embryo at the pre-streak (left), early-streak (middle) or mid-streak (right) stage of gastrulation. The position of sections within the intact embryo is illustrated in supplementary material Fig. S1A; posterior is at the top. The primitive streak (PS) region in the early- and mid-streak images is outlined (dashed line). Brachyury (A-A″, green), Tcf7l1 (B-B″, green), Oct4 (C-C″, cyan) and Sox2 (D-D″, yellow) are shown with co-staining for E-cadherin (magenta). The domain of Nanog immunoreactivity (E-E″, green) is marked by a solid yellow outline. (**F-J**) The levels of protein immunoreactivity in individual cells relative to their position in the epiblast, as described in supplementary material Fig. S1C. The intensity of immunoreactivity in individual epiblast nuclei (*y*-axis) is compared with distance from the PS (*x*-axis). The number of nuclei analyzed (*n*) and Pearson correlation coefficients (*r*) are listed for each. **P*<10^{-5}, ***P*<10^{-10}.

embryos (Fig. 1C-C″). Oct4 protein was also detected in the nascent mesoderm cells of mid-streak embryos (Fig. 1C″), indicating that it does not need to be lost for mesoderm specification. Sox2 protein was slightly decreased at the posterior of the pre-streak epiblast (Fig. 1D), where a low level of Nanog protein was also detected (Fig. 1E). The opposing expression patterns of Nanog and Sox2 intensify during progression through the early-streak and mid-streak stages as Sox2 levels decrease (Fig. 1D′,D″) and Nanog levels increase (Fig. 1E′,E″) at the PS.

To provide a complementary analysis of pluripotency factor dynamics prior to lineage specification, we measured levels of protein immunofluorescence in individual epiblast cells of early-streak embryos. Labeling experiments showed that lateral cells of the proximal epiblast move towards and enter the PS region (Lawson et al., 1991) (supplementary material Fig. S1B). Thus, the correlation between protein expression patterns and the distance of a cell from the PS can be used to represent the protein expression changes that occur in epiblast cells as they move towards the PS. Early-streak embryos were chosen for analysis because they have just initiated mesoderm specification at the PS. Brachyury showed the expected strong negative correlation with distance from the PS (*r*=–0.74), as brachyury was expressed only in epiblast cells near the PS (Fig. 1F). Both Tcf7l1 and Sox2 showed a strong positive correlation (*r*=0.60 and *r*=0.65), whereas Oct4 expression did not appear to change near the PS (*r*=0.32) (Fig. 1G-I). Like brachyury, Nanog expression showed a strong negative correlation with distance from the PS (*r*=–0.72); however, Nanog was expressed in a broader posterior domain of epiblast cells (Fig. 1J). This indicated that Nanog is expressed prior to brachyury as cells move towards the PS, a conclusion supported by double immunofluorescence staining (supplementary material Fig. S1C). Taken together, these data indicate that, as epiblast cells move towards the PS, they undergo gene expression changes through which Nanog expression is increased and Tcf7l1 and Sox2 are downregulated.

Tcf7l1 accelerates the dynamics of pluripotency factor expression during gastrulation

Unlike embryos genetically lacking *Oct4*, *Sox2* or *Nanog* gene products, *Tcf7l1*$^{-/-}$ embryos survive implantation and undergo gastrulation (Avilion et al., 2003; Merrill et al., 2004; Mitsui et al., 2003; Nichols et al., 1998). Ablation of *Tcf7l1* on a mixed genetic background (C57BL/6/129Sv) generated a broad range of morphogenetic defects that were phenotypically classified into two groups (mildly and severely affected) occurring at roughly equal frequency (48% and 52%, respectively) (Merrill et al., 2004). In this mixed background, mesoderm markers displayed a variety of abnormal expression patterns in mutants; the earliest defects were reported for E7.0 embryos and included reduced brachyury (Merrill et al., 2004). We reasoned that the variable expressivity would complicate analysis of gene expression in *Tcf7l1*$^{-/-}$ epiblasts and sought to reduce variability. Repeated backcrosses (>20 generations) produced a *Tcf7l1*$^{+/-}$ strain congenic for C57BL/6, from which greater than 95% of *Tcf7l1*$^{-/-}$ embryos displayed the previously described severe phenotype (Merrill et al., 2004). Although the genetic determinants influencing the *Tcf7l1*$^{-/-}$ phenotype remain unknown, the uniformity of the *Tcf7l1*$^{-/-}$ phenotype permitted faithful examination of pluripotency factor expression among mutant embryos.

Analysis of pluripotency factor expression in *Tcf7l1*$^{-/-}$ blastocysts and E5.5 embryos indicated no significant differences relative to *Tcf7l1*$^{+}$ (either *Tcf7l1*$^{+/+}$ or *Tcf7l1*$^{+/-}$) embryos (supplementary material Fig. S2A,B). Differences were first detected at E6.5, as the level of *Nanog* mRNA was significantly increased in *Tcf7l1*$^{-/-}$ embryos (Fig. 2A). By contrast, *Oct4* mRNA levels were not increased in *Tcf7l1*$^{-/-}$ embryos (Fig. 2A), which is consistent with weak direct effects of Tcf7l1 ablation on Oct4 expression in ESCs (Pereira et al., 2006; Yi et al., 2008). The domain of *Nanog* mRNA expression was expanded to the anterior of *Tcf7l1*$^{-/-}$ embryos (Fig. 2B).

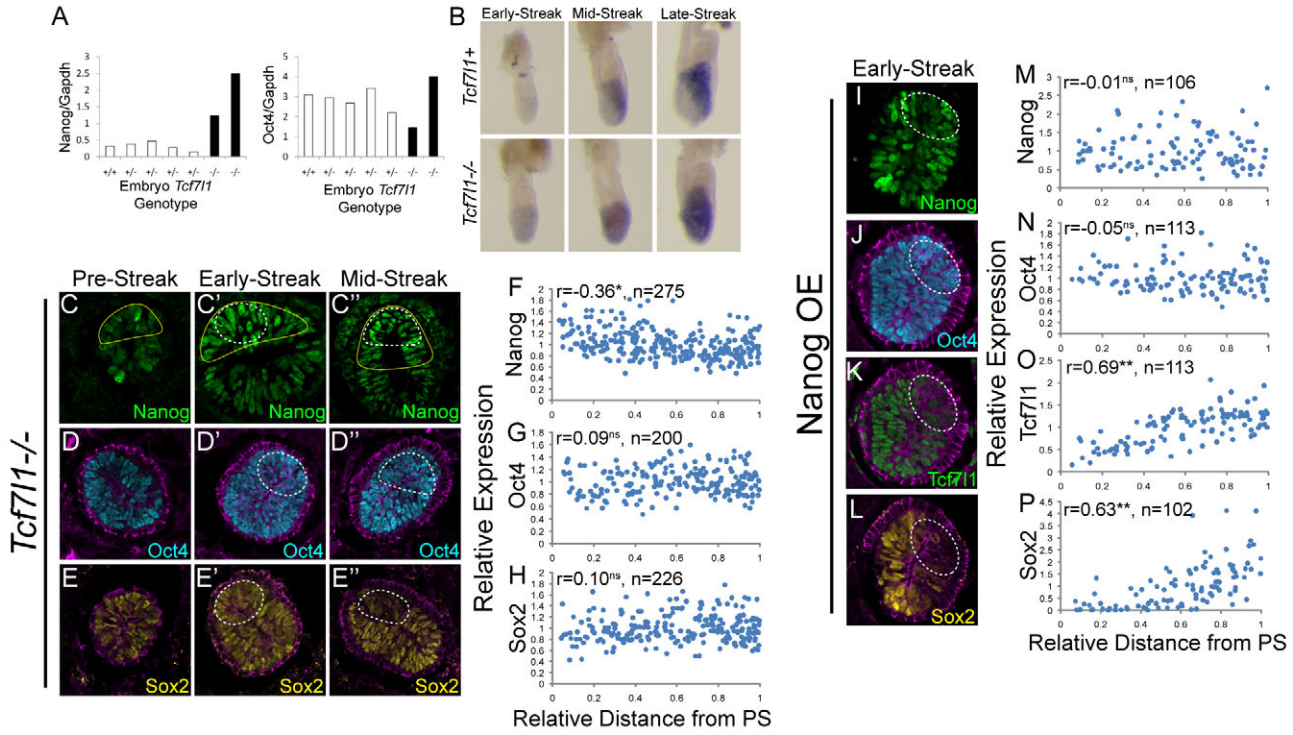

Fig. 2. Tcf7l1 is necessary for dynamic expression of pluripotency factors in the epiblast. (**A**) Quantitative RT-PCR assays measuring *Nanog* and *Oct4* RNA levels relative to *Gapdh* from individual early-streak mouse embryos. The *Tcf7l1* genotype of each embryo is indicated beneath each bar; *Tcf7l1*$^{-/-}$ bars are black. (**B**) Whole-mount *in situ* hybridization analysis of *Nanog* mRNA expression in early-, mid- and late-streak *Tcf7l1*$^{+}$ and *Tcf7l1*$^{-/-}$ embryos. Lateral views are shown; posterior is to the right. (**C-E″**) Immunofluorescent staining of transverse cryosections of *Tcf7l1*$^{-/-}$ embryos for Nanog (C-C″, green), Oct4 (D-D″, cyan) and Sox2 (E-E″, yellow). The position of sections within the intact embryo is illustrated in supplementary material Fig. S1A; posterior is at the top. The PS region in the early- and mid-streak images is outlined (dashed line). The solid yellow outline of Nanog expression in *Tcf7l1*$^{+}$ embryos (see Fig. 1E-E″) is overlaid on *Tcf7l1*$^{-/-}$ embryos (C-C″) for comparison. (**F-H**) Quantitation of protein immunoreactivity in early-streak stage *Tcf7l1*$^{-/-}$ embryos. (**I-L**) Immunofluorescent staining of transverse cryosections of early-streak stage Nanog-overexpressing embryos for Nanog (I, green), Oct4 (J, blue), Tcf7l1 (K, green) and Sox2 (L, yellow). (**M-P**) Quantitation of protein immunoreactivity in early-streak stage Nanog-overexpressing embryos. Protein immunoreactivity was quantitated as described in Fig. 1F-J and supplementary material Fig. S1C.

To determine whether Tcf7l1 affected the dynamics of pluripotency protein expression during PS formation, we analyzed immunoreactivity in *Tcf7l1*$^{-/-}$ embryos as described above for wild-type embryos (Fig. 1). The most substantial effect was on Nanog protein, which was detected in every cell of *Tcf7l1*$^{-/-}$ epiblasts at pre-, early- and mid-streak stages (Fig. 2C-C″; supplementary material Fig. S3B-E) but not in E5.5 embryos (supplementary material Fig. S2B). Oct4 levels were uniform throughout the *Tcf7l1*$^{-/-}$ epiblast (Fig. 2D-D″). Sox2 protein levels remained uniform in *Tcf7l1*$^{-/-}$ pre-streak and early-streak embryos (Fig. 2E,E′), and reduction of Sox2 protein at the PS region did not occur in *Tcf7l1*$^{-/-}$ embryos until the mid-streak stage (Fig. 2E″). Comparison of relative factor levels with position in early-streak *Tcf7l1*$^{-/-}$ embryos showed a weak negative correlation for Nanog (r=–0.36) and no significant correlation for Oct4 (r=0.09) or Sox2 (r=0.10) (Fig. 2F-H). Comparing patterns in *Tcf7l1*$^{-/-}$ and *Tcf7l1*$^{+/+}$ epiblasts shows that Tcf7l1 is necessary for the changes to Nanog and Sox2 expression in epiblast cells as they move towards the PS to undergo lineage specification (supplementary material Fig. S1D,E).

Given the ability of Nanog to stimulate self-renewal *in vitro* and the repression of *Nanog* promoter activity by Tcf7l1 (Chambers et al., 2003; Mitsui et al., 2003; Pereira et al., 2006), we tested whether dysregulated Nanog is sufficient to cause a *Tcf7l1*$^{-/-}$ phenotype by engineering a doxycycline-inducible *Nanog* transgenic mouse (supplementary material Fig. S4). Induction of Nanog overexpression in transgenic embryos generated an expansion of Nanog expression similar in timing and pattern to the dysregulated Nanog expression in *Tcf7l1*$^{-/-}$ embryos (compare Fig. 2I with 2C′; supplementary material Fig. S4E). The patterns of *Oct4*, *Sox2* and *Tcf7l1* gene expression (Fig. 2J-P) were indistinguishable from those observed in transgenic embryos lacking Nanog overexpression (supplementary material Fig. S5) and in wild-type embryos (Fig. 1B-D″,G-I). Thus, the role of Tcf7l1 in the epiblast extends beyond the regulation of Nanog expression.

Tcf7l1 is necessary for maturation of the epiblast during gastrulation

Recent work showed that pluripotency, as assessed by the ability of cells to form EpiSCs, is lost from mouse embryos between E7.5 and E8.25 (Osorno et al., 2012). This coincides with the reduction of *Oct4* and *Nanog* mRNA, which begin declining at E7.5 and are undetectable by E8.5 (Fig. 3A-E) (Osorno et al., 2012). In *Tcf7l1*$^{-/-}$ embryos, *Nanog* and *Oct4* mRNAs were expressed at high levels throughout the embryonic ectoderm through E8.5 (Fig. 3A′-E′). Otx2 is another marker of epiblast progression and has recently been shown to stabilize an epiblast-like state (Acampora et al., 2013). *Otx2* mRNA is uniformly expressed throughout the early epiblast and becomes progressively restricted to the anterior neuroectoderm by E7.5 in wild-type embryos (Fig. 3F). In *Tcf7l1*$^{-/-}$ embryos, Otx2

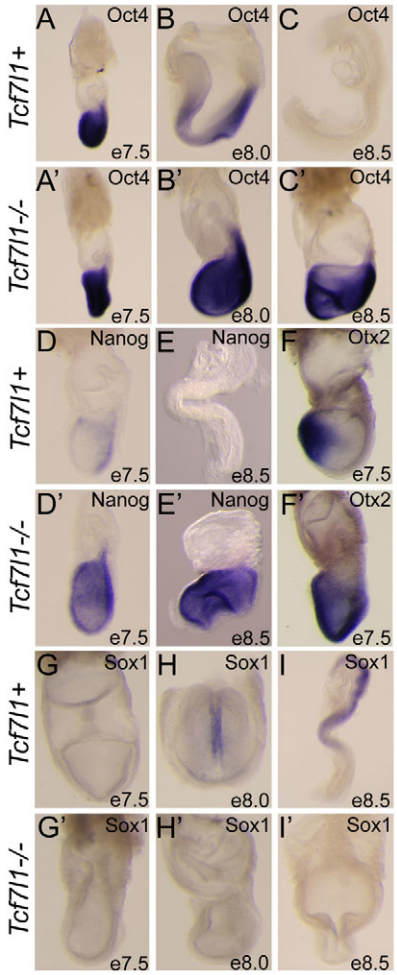

Fig. 3. Tcf7l1 is required for silencing of pluripotency factor expression and early neurectoderm specification. (**A-I′**) Whole-mount *in situ* hybridization for *Oct4* (A-C′), *Nanog* (D-E′), *Otx2* (F,F′) and *Sox1* (G-I′) in *Tcf7l1*$^{+}$ (A-I) and *Tcf7l1*$^{-/-}$ (A′-I′) mouse embryos of the indicates ages. Lateral views, except for frontal views in G,G′,H,H′,I′.

expression persisted throughout the entire E7.5 epiblast (Fig. 3F′). Severely affected E8.5 *Tcf7l1*$^{-/-}$ embryos lacked morphological signs of neural fold formation, which is typically complete by this time (Fig. 3) (Merrill et al., 2004). The early neuroectoderm marker Sox1 is induced by E8.0 and rapidly intensifies from E8.0 to E8.5 during neuroectoderm differentiation in wild-type embryos (Fig. 3G-I). In *Tcf7l1*$^{-/-}$ mutants, *Sox1* mRNA was not detectable through E8.5 (Fig. 3G′-I). The abnormal morphology and altered patterns of gene expression indicated that neural specification is defective in epiblast cells lacking Tcf7l1, and that the *Tcf7l1*$^{-/-}$ epiblast retained characteristics of earlier epiblast stages for a prolonged period.

Coupling of mesoderm specification and primitive streak induction requires Tcf7l1

We next tested the hypothesis that effects of Tcf7l1 in the epiblast are important in preparing cells for lineage specification. In normal mouse embryos, the timing of mesoderm specification occurs concomitantly with the formation of the PS. Therefore, examining the onset of mesoderm specification in *Tcf7l1*$^{-/-}$ embryos presented the possibility of identifying a novel role in coordinating cell fates with morphogenesis. However, the rapid formation of the PS during gastrulation generates substantial variability in developmental stage between individual embryos in a single litter (Downs and Davies, 1993; Rivera-Pérez et al., 2010), and distinct markers have not been identified in the mouse to separate the specification of mesoderm from the induction of morphological PS formation. In chickens, inhibition of the Wnt planar cell polarity (PCP) pathway blocked cell movement in the PS without inhibiting mesoderm gene expression (Voiculescu et al., 2007). Thus, the PCP pathway is specifically required for PS morphogenesis and not for lineage specification at the PS. The PCP pathway gene *Prickle1* was previously shown to be expressed in gastrulation stage embryos (Crompton et al., 2007), indicating its potential utility as a marker of morphological PS formation. Indeed, the timing and pattern of *Prickle1* mRNA expression in the epiblast are very similar to those of brachyury protein expression (Fig. 4A). Therefore, we examined the coordination of brachyury and Prickle1 expression in individual embryos by generating arrays of cryosections such that several assays could be performed on adjacent sections throughout the proximodistal length of individual embryos.

Perfect coordination of *Prickle1* mRNA and brachyury protein expression at the onset of PS formation was apparent in all *Tcf7l1*$^{+}$ embryos (Fig. 4B; n=43 of 43), and we never observed *Tcf7l1*$^{+}$ embryos that expressed Prickle1 without coincident brachyury expression in adjacent sections. Mixl1 expression, another early marker of mesoderm lineage specification, was also perfectly coupled with Prickle1 expression in *Tcf7l1*$^{+}$ embryos (Fig. 4D). Thus, Prickle1 served as a valuable marker to stage embryos and determine whether mesendoderm lineage specification should be detectable. In *Tcf7l1*$^{-/-}$ embryos defined as early-streak stage based on the presence of Prickle1 expression in the posterior epiblast, the expression of brachyury, Mixl1 and Gsc was strikingly absent in adjacent sections (Fig. 4C, n=16 of 16; Fig. 4E, n=6 of 6; supplementary material Fig. S6A,A′, n=3 of 3). This demonstrated that mesendoderm specification was uncoupled from PS formation in *Tcf7l1*$^{-/-}$ embryos. Brachyury and Mixl1 expression and mesenchymal mesoderm cell types were all apparent in later stage *Tcf7l1*$^{-/-}$ embryos (supplementary material Fig. S6B-C′) (Merrill et al., 2004; Wu et al., 2012). Formation of mesoderm cells indicates that Tcf7l1 is not necessary for the specification of mesoderm per se, but it is specifically needed for the initial response of epiblast cells to lineage specification signals. Taken together with normal Prickle1 expression in *Tcf7l1*$^{-/-}$ embryos, these data demonstrated that, rather than an overall delay in gastrulation, *Tcf7l1*$^{-/-}$ epiblast cells exhibit delayed mesendoderm specification relative to the induction of the PS, thus uncoupling these two tightly linked processes.

Tcf/Lef-β-catenin activation of target genes, including brachyury, has been associated with mesendoderm gene expression at the PS (Arnold et al., 2000; Galceran et al., 2001). Although mesendoderm gene expression occurred in later stage *Tcf7l1*$^{-/-}$ embryos (supplementary material Fig. S6C,C′) (Merrill et al., 2004; Wu et al., 2012), it was formally possible that Tcf7l1 could be required to stimulate initial lineage specification through Tcf7l1-β-catenin complexes. To test this possibility, we used the *Tcf7l1*$^{\Delta N/\Delta N}$ knock-in mouse, in which the Tcf7l1-β-catenin interaction is ablated (Wu et al., 2012). *Tcf7l1*$^{\Delta N/\Delta N}$ embryos displayed perfectly coupled brachyury and Prickle1 expression (Fig. 4F), indicating that Tcf7l1-β-catenin is not necessary for timely mesoderm specification during PS formation. *Tcf7l1*$^{\Delta N/\Delta N}$ embryos also exhibited normal expression of Nanog (supplementary material Fig. S6D,D′) and proper restriction of Otx2 expression in the E7.5 epiblast (supplementary material Fig. S6D″). Finally, the expression of the Wnt-β-catenin

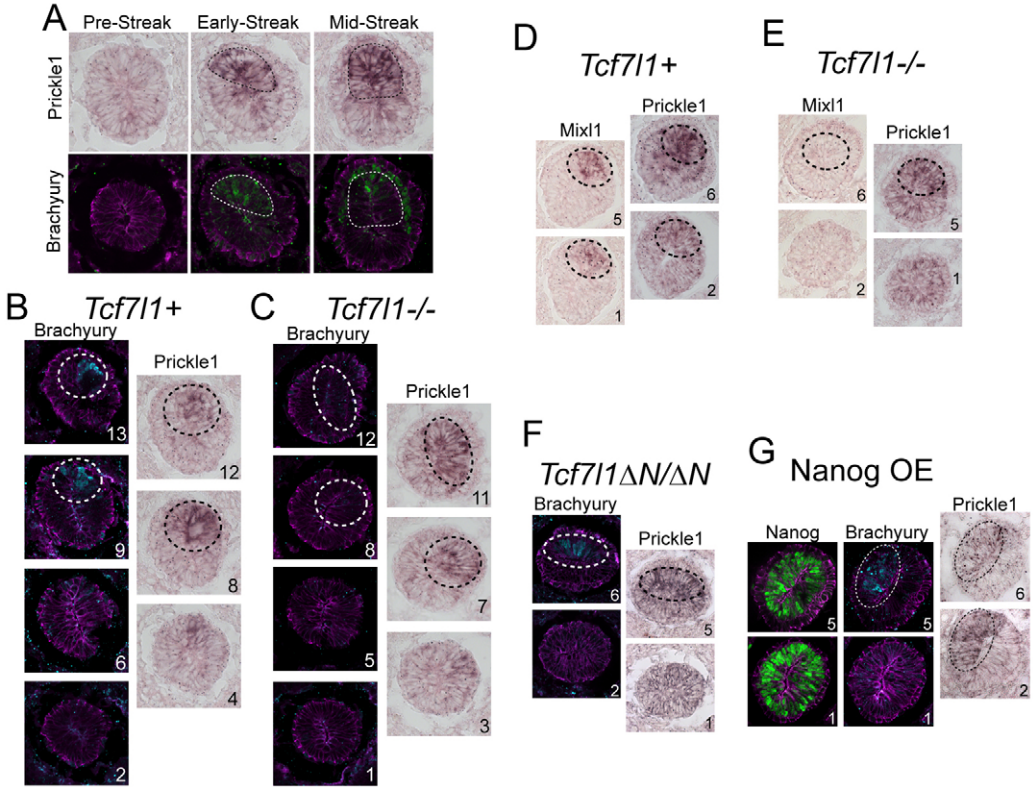

Fig. 4. Coupling mesoderm specification to primitive streak formation requires Tcf7l1. (**A**) *In situ* hybridization for *Prickle1* mRNA (top row, purple) and immunofluorescent detection of brachyury protein (bottom row, green) and E-cadherin (bottom row, magenta) in transverse sections of pre-, early- and mid-streak stage mouse embryos. The PS region is outlined (dashed line). (B-G) Each image shows assays from an individual early-streak stage embryo. Numbers (bottom right) indicate the position of each section relative to the most distal (#1) section pictured for each embryo. (**B**,**C**) Brachyury (cyan) and E-cadherin (magenta) protein immunoreactivity and *Prickle1* mRNA *in situ* hybridization for *Tcf7l1*$^{+}$ (B) and *Tcf7l1*$^{-/-}$ (C) embryos. (**D**,**E**) *Mixl1* and *Prickle1* mRNA *in situ* hybridization assays for *Tcf7l1*$^{+}$ (D) and *Tcf7l1*$^{-/-}$ (E) embryos. (**F**) Brachyury (cyan) and E-cadherin (magenta) protein immunoreactivity and *Prickle1* mRNA *in situ* hybridization for a *Tcf7l1*$^{\Delta N/\Delta N}$ embryo. (**G**) Nanog (green), brachyury (cyan) and E-cadherin (magenta) protein immunoreactivity and *Prickle1* mRNA *in situ* hybridization for a Nanog-overexpressing transgenic embryo.

target gene *Axin2* was indistinguishable between *Tcf7l1*$^{+}$, *Tcf7l1*$^{-/-}$ and *Tcf7l1*$^{\Delta N/\Delta N}$ embryos (supplementary material Fig. S6E). Together, these data indicated that the requirement for Tcf7l1 in the epiblast was independent of its interaction with β-catenin.

Forced Nanog expression is sufficient to block lineage specification in ESCs (Chambers et al., 2003; Mitsui et al., 2003; Thomson et al., 2011). We used Nanog-overexpressing transgenic embryos to test whether expanded expression of Nanog was responsible for the delayed mesoderm lineage specification in *Tcf7l1*$^{-/-}$ embryos. Of 18 Nanog-overexpressing embryos examined, 17 had coupled brachyury and Prickle1 expression indistinguishable from non-expressing controls (Fig. 4G). Thus, recapitulating Nanog dysregulation was not sufficient to disturb the dynamics of pluripotency factor expression (Fig. 2I-P) or to cause a significant delay in mesoderm specification.

Tcf7l1 stimulates a switch in the response to Wnt/β-catenin signaling from self-renewal to mesoderm specification

To determine the mechanism underlying the delayed mesoderm specification in *Tcf7l1*$^{-/-}$ embryos, we examined the transition from naïve to primed states of pluripotency *in vitro*. When switched to EpiSC culture conditions (serum-free N2B27 media with Fgf2 and activin A), naïve ESCs rapidly adopt a primed EpiSC morphology, exhibit reduced alkaline phosphatase (AP) activity and lose the ability to self-renew as naïve ESCs (Guo and Smith, 2010; Rugg-Gunn et al., 2012). After 3 days of EpiSC conditions (Fig. 5A), nearly all *Tcf7l1*$^{+/+}$ colonies (98%) exhibited an AP-negative EpiSC-like morphology (Fig. 5B). Conversely, less than half of *Tcf7l1*$^{-/-}$ colonies (48%) formed AP-negative EpiSC-like colonies after 3 days (Fig. 5B).

To measure the commitment to a primed state after 3 days in EpiSC conditions, colonies were dissociated into single cells, replated in ESC conditions and assayed for AP-positive ESC-like colonies after 4 days. Few (2.0±1.4) ESC colony-forming units (CFU) were recovered per 1000 *Tcf7l1*$^{+/+}$ cells replated (Fig. 5C), consistent with previous observations that EpiSCs do not readily revert to the naïve ESC state (Bernemann et al., 2011; Guo and Smith, 2010). By contrast, the number of ESC CFU (36±2.8) was significantly greater from replated *Tcf7l1*$^{-/-}$ cells (Fig. 5C), indicating that more *Tcf7l1*$^{-/-}$ cells retained the capacity to self-renew as ESCs. This resistance to priming was temporary for *Tcf7l1*$^{-/-}$ ESCs, as nearly all *Tcf7l1*$^{-/-}$ colonies exhibited an AP-negative EpiSC-like morphology after 5 days in EpiSC conditions (supplementary material Fig. S7A).

The expression of several genes differs between naïve ESCs and primed EpiSCs. Whereas *Oct4* is typically expressed at similar levels in ESCs and EpiSCs, *Nanog*, *Sox2* and other markers of the

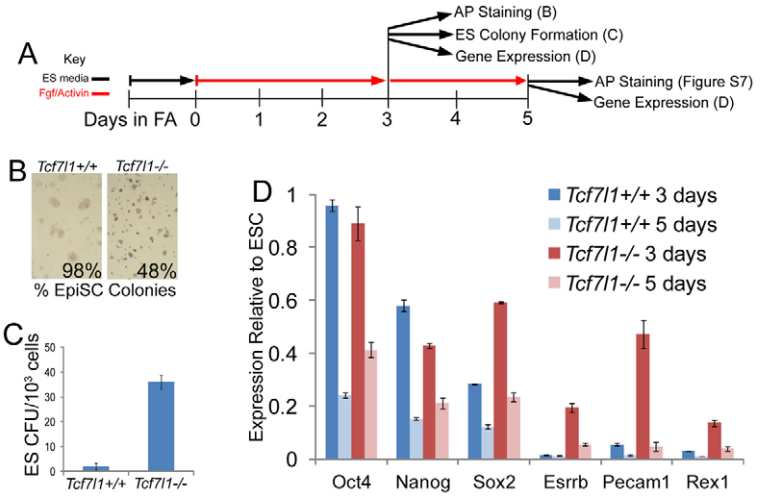

Fig. 5. Tcf7l1 is necessary for timely transition of ESCs to the EpiSC state. (**A**) Experimental design. ESCs were plated in ESC media for 24 hours and switched to EpiSC (FA) media at day 0. After 3 days in EpiSC conditions, samples were either cultured for 2 additional days or prepared for alkaline phosphatase (AP) staining, ESC colony formation assays and gene expression analysis. (**B**) Representative images of AP staining of *Tcf7l1*$^{+/+}$ and *Tcf7l1*$^{-/-}$ cells grown in EpiSC conditions for 3 days. The percentage of colonies with an EpiSC-like morphology is indicated. (**C**) Number of ESC colony-forming units (CFU) per 1000 cells after 3 days of culture in EpiSC conditions. (**D**) Quantitative RT-PCR assays measuring the levels of core pluripotency genes (*Oct4*, *Nanog* and *Sox2*) and naïve state genes (*Esrrb*, *Pecam1* and *Rex1*) after 3 or 5 days in EpiSC conditions. Values are normalized to the level of expression of each gene in *Tcf7l1*$^{+/+}$ ESCs. Error bars indicate s.d. between biological replicates.

naïve state [*Esrrb*, *Pecam1*, *Rex1* (*Zfp42* – Mouse Genome Informatics)] are expressed at far lower levels in EpiSCs, and epiblast-specific genes (*Fgf5*, *Dnmt3b*) are expressed at much higher levels (Brons et al., 2007; Greber et al., 2010; Tesar et al., 2007). Indeed, after 3 days in EpiSC conditions, *Fgf5* and *Dnmt3b* were increased whereas *Nanog*, *Sox2*, *Esrrb*, *Pecam1* and *Rex1* levels were reduced in both *Tcf7l1*$^{+/+}$ and *Tcf7l1*$^{-/-}$ cells (Fig. 5D; supplementary material Fig. S7B). However, the reduction of the naïve markers *Esrrb*, *Pecam1* and *Rex1* was significantly less substantial in *Tcf7l1*$^{-/-}$ cells (Fig. 5D). After an additional 2 days in EpiSC conditions, *Sox2*, *Esrrb*, *Pecam1* and *Rex1* were further decreased in *Tcf7l1*$^{-/-}$ to levels similar to those in *Tcf7l1*$^{+/+}$ cells after 3 days in EpiSC conditions (Fig. 5D). Somewhat surprisingly, *Oct4* levels decreased in both *Tcf7l1*$^{+/+}$ and *Tcf7l1*$^{-/-}$ cultures after 5 days in EpiSC conditions (Fig. 5D). This is likely to indicate some level of conversion to a later epiblast state and that differentiation

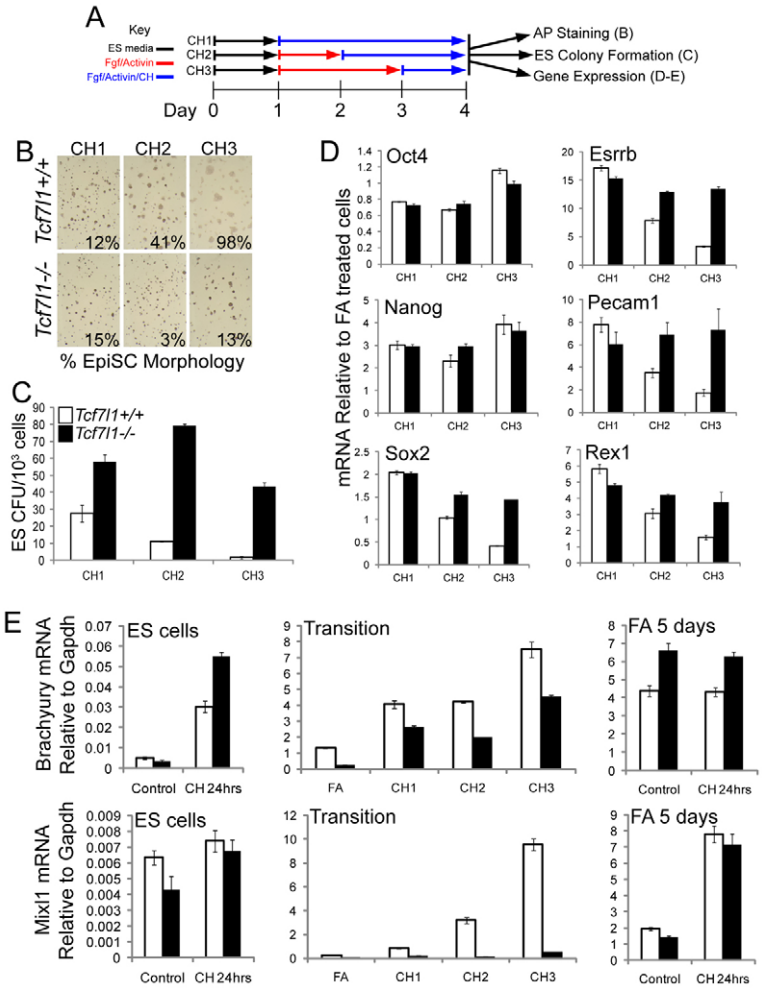

Fig. 6. Tcf7l1 is necessary for the switch from self-renewal to mesoderm specification in response to Wnt/β-catenin signaling in pluripotent stem cells. (**A**) Experimental design. ESCs were plated in ESC media and switched to EpiSC (FA) media at day 1. The Gsk3 inhibitor CHIR99021 (CH) was added to media to activate Wnt/β-catenin signaling at either day 1 (CH1), day 2 (CH2) or day 3 (CH3). After 3 days in the CH1-3 regimens, samples were prepared for AP staining and assessment of colony morphology (B), ESC colony formation assays (C) and gene expression analysis (D,E). (**B**) AP staining of colonies after completing CH1-3 regimens. The percentage of colonies displaying an EpiSC morphology with low AP activity is shown. (C-E) *Tcf7l1*$^{+/+}$ is depicted by white bars, *Tcf7l1*$^{-/-}$ by black bars. (**C**) Number of ESC CFU per 1000 cells after completing the CH1-3 regimens. (**D**) Quantitative RT-PCR assays measuring the levels of core pluripotency genes (*Oct4*, *Nanog* and *Sox2*) and naïve state genes (*Esrrb*, *Pecam1* and *Rex1*) after completing CH1-3 regimens. Values are normalized to the level of expression of each gene in *Tcf7l1*$^{+/+}$ cells cultured in EpiSC media without CH. (**E**) Quantitative RT-PCR assays measuring the levels of the mesoderm genes brachyury (top) and *Mixl1* (bottom) in response to CH in ESCs (left), in cells undergoing transition (as diagramed in A) (middle), and in cells after 5 days of culture in EpiSC conditions (right). Values are normalized to the level of *Gapdh* expression in each sample. Error bars indicate s.d. between biological replicates.

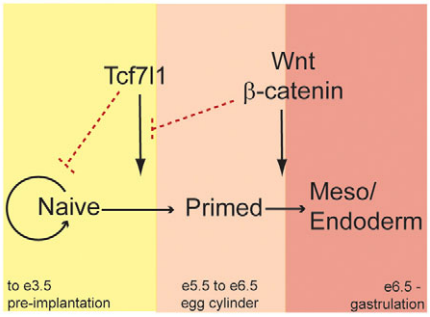

Fig. 7. Model depicting the effects of Tcf7l1 and Wnt/β-catenin on pluripotent cells in mice. As cells progress from naïve pluripotency (yellow; ESC, preimplantation epiblast) to a primed state (pink; EpiSC, postimplantation epiblast) they acquire the ability to form mesoderm in response to Wnt/β-catenin. Tcf7l1 mediates the transition from the naïve to the primed state. Wnt/β-catenin inhibits this transition.

is occurring in this assay, consistent with decreased Oct4 in EpiSCs derived from E6.5 epiblasts compared with E5.5 epiblasts (Bernemann et al., 2011). Together, these data indicate that, in the absence of Tcf7l1, ESCs were delayed, but not completely blocked, in transitioning to a primed, epiblast-like state when subjected to EpiSC conditions. This *in vitro* delay was consistent with Tcf7l1 repressing naïve ESC self-renewal and consistent with a function of Wnt/β-catenin in maintaining a naïve state (ten Berge et al., 2011).

Wnt/β-catenin clearly stimulates self-renewal of mouse ESCs, i.e. cells in a naïve state (ten Berge et al., 2011; Sato et al., 2004; Ying et al., 2008). Conversely, activation of Wnt signaling in EpiSCs by addition of the Gsk3 inhibitor CHIR99021 (CH) promotes mesendoderm and extra-embryonic differentiation (Greber et al., 2010). Furthermore, recent reports indicate that Wnt/β-catenin stimulates mesoderm specification of human ESCs, i.e. cells considered to be in a primed state (Davidson et al., 2012; Singh et al., 2012). We reasoned that the differences in these responses to Wnt/β-catenin could be dependent on the transition from naïve to primed pluripotency. To test this, we activated Wnt/β-catenin signaling at 24-hour intervals after switching from ESC to EpiSC conditions (Fig. 6A) to identify the point at which the cellular response to Wnt/β-catenin switches from self-renewal to mesoderm specification. CH was used to stimulate Wnt/β-catenin signaling because of its ability to activate the pathway regardless of changes to Wnt-receptor complexes that may occur during the transition.

When CH was added immediately upon switching cells to EpiSC conditions (CH1), *Tcf7l1*$^{+/+}$ colonies maintained an ESC-like morphology (Fig. 6B), the ability to self-renew in ESC conditions (Fig. 6C) and naïve gene expression (Fig. 6D). When CH was added 24 or 48 hours (CH2 and CH3) after switching to EpiSC conditions, its effectiveness in maintaining ESC-like characteristics progressively diminished (Fig. 6B-D). Thus, CH inhibited the transition to the primed state, but this ability was limited to a short window of time at the beginning of the transition. Like *Tcf7l1*$^{+/+}$ cells, *Tcf7l1*$^{-/-}$ cells cultured in the CH1 regimen exhibited enhanced ESC characteristics (Fig. 6B-D). However, unlike *Tcf7l1*$^{+/+}$, the maintenance of ESC-like morphology and gene expression by CH was not attenuated in *Tcf7l1*$^{-/-}$ cells in the CH2 or CH3 regimen (Fig. 6B,C). Thus, the window during which CH could inhibit the transition to the primed state was expanded by the absence of Tcf7l1.

To determine whether Tcf7l1 regulation of the transition to the primed state affected mesendoderm specification, we measured the expression of brachyury, *Mixl1*, *Gsc* and *Foxa2*. Prior to transitioning to a primed state, ESCs expressed very low levels of these genes, and CH did not stimulate *Mixl1*, *Gsc* or *Foxa2* expression in either *Tcf7l1*$^{+/+}$ or *Tcf7l1*$^{-/-}$ ESCs (Fig. 6E; supplementary material Fig. S7C; left). Brachyury expression was increased by CH in ESCs (Fig. 6E, left). Each gene was expressed at much lower levels (~100- to 1000-fold) in ESCs compared with cells subjected to 5 days of EpiSC conditions (Fig. 6E; supplementary material Fig. S7C; right), indicating that mesoderm specification is dependent on transition to the primed state. The notable point is that, both before and after the transition to a late epiblast state, *Tcf7l1*$^{+/+}$ and *Tcf7l1*$^{-/-}$ cells expressed similar levels of mesoderm marker genes and exhibited similar responses to CH. Thus, Tcf7l1 was not necessary for mesendoderm gene expression in cells that had acquired characteristics of late epiblast cells. By contrast, *Tcf7l1*$^{-/-}$ cells exhibited markedly reduced mesendoderm gene expression in response to CH during the transition between states (Fig. 6E; supplementary material Fig. S7C; middle). The effect was strongest for *Mixl1* and *Gsc*, which effectively were not induced in *Tcf7l1*$^{-/-}$ cells until 5 days of culture in EpiSC media was complete. Taken together with the effects on naïve cell characteristics (Fig. 6B-D), these results show that Tcf7l1 stimulates a rapid transition to a primed state, which is necessary for the response to mesendoderm specification signals.

DISCUSSION

The activity of Tcf7l1 as a transcriptional repressor is integrated into the Oct4/Sox2/Nanog GRN (Cole et al., 2008; Marson et al., 2008; Yi et al., 2008). Tcf7l1-repression of the *Esrrb* gene (Martello et al., 2012) further emphasizes that Tcf7l1 functions in ESCs as an intrinsic inhibitor of pluripotent cell self-renewal. By contrast, an *in vivo* function for the repressor activity of Tcf7l1 in pluripotency was not clear. In particular, it was remarkable that this inhibitor of pluripotent cell self-renewal was expressed at high levels in pluripotent cells, rendering them dependent on Wnt/β-catenin activity *in vitro* (ten Berge et al., 2011; Wray et al., 2011; Yi et al., 2011). The work presented here provides a new understanding of the *in vivo* role of Tcf7l1 in pluripotent cells by showing that Tcf7l1 is needed for pluripotent cells to be properly prepared for lineage specification in response to differentiation stimuli (Fig. 7). This activity of Tcf7l1 is needed for the specification of mesoderm from pluripotent epiblast cells to be coupled with the induction of the PS during gastrulation.

In considering the importance of the coupling function, one must distinguish the consequences of an uncoupling effect from those of simply slowing down embryogenesis. An overall slowing of embryonic events does not necessarily cause significant effects. Indeed, early mouse embryos can suspend development for a period of days in a process called diapause, and then return to normal embryogenesis (Renfree and Shaw, 2000). By contrast, uncoupling PS induction and mesoderm specification disrupts the normal sequence of events that occur during gastrulation. Given the dynamics of gastrulation, when epiblast cells divide frequently (~10-hour doubling time) (Snow, 1977) and require less than 24 hours to enter the PS, become mesoderm and migrate away from the PS (Lawson et al., 1991), it seems likely that an uncoupling event resulting in a delay of only a few hours would nonetheless have substantial downstream effects. After delayed mesoderm specification at E6.5-6.75, *Tcf7l1*$^{-/-}$ embryos display a number of patterning defects, including ectopic axial mesoderm at the expense

of paraxial and lateral mesoderm lineages, the appearance of partial duplications to the primary body axis by E7.5 (Merrill et al., 2004), and a lack of neuroectoderm specification (Fig. 3). Although not directly tested, it is likely that these patterning defects in *Tcf7l1*$^{-/-}$ embryos are secondary to the uncoupling, and that coordinating mesoderm specification with the induction of the PS is the crucial embryonic function of Tcf7l1.

To elucidate a cellular mechanism underlying the delayed mesoderm specification in *Tcf7l1*$^{-/-}$ embryos, a combination of stem cell culture and embryo experiments was conducted. These experiments provide a good opportunity to assess the similarities and differences between the two systems with respect to lineage specification. Some *in vitro* effects occur similarly in ESCs and embryos; reduction of Sox2 precedes mesoderm specification of ESCs in response to activation of Wnt signaling by CH (Thomson et al., 2011) as well as in the PS region of the epiblast (Fig. 1D). This role appears to be broadly conserved, as SoxB1 proteins also regulate lineage specification events in chicken and *Xenopus* embryos and inhibit mesendoderm differentiation in human ESCs (Acloque et al., 2011; Shih et al., 2010; Wang et al., 2012). The transcriptional repressor activity of Tcf7l1 on the *Nanog* promoter described in ESCs also appears to function in the epiblast during gastrulation (Pereira et al., 2006). By contrast, ESC differentiation has been shown to be sensitive to Oct4 and Nanog levels (Nichols et al., 1998; Niwa et al., 2000; Chambers et al., 2003; Mitsui et al., 2003; Thomson et al., 2011); however, Oct4 protein immunoreactivity was uniform throughout the pre-streak to late-streak epiblast and Nanog protein levels actually increased in epiblast cells as they moved towards the PS. Moreover, forced expression of Nanog in the epiblast had no apparent effect on lineage specification. We propose that these inconsistencies are due to the different pluripotent states of ESCs and postimplantation epiblast cells. These observations highlight the need for a greater understanding of the different states of pluripotency for broadly comparing mechanisms of *in vitro* and *in vivo* lineage specification.

At precisely what stage of development is Tcf7l1 repressor activity needed? Tcf7l1 had little effect on mesoderm gene expression in cells that were kept in a naïve state (i.e. self-renewing ESCs) and cells that had already progressed to a primed state (i.e. cells cultured for 5 days in EpiSC conditions). The primary effect of Tcf7l1 was apparent only as cells transitioned from a naïve to primed state. Analysis of heterogeneity within EpiSC cultures and differences between lines of EpiSCs shows that primed cells can exist in multiple metastable states (Bernemann et al., 2011; Han et al., 2010). Compared with earlier states, later states of primed cells express higher levels of brachyury and are more resistant to reversion back to a naïve state (Bernemann et al., 2011). Based on the retention of ESC colony-forming potential of *Tcf7l1*$^{-/-}$ cells in EpiSC media, we suggest that Tcf7l1 is necessary for a relatively early stage of the priming process. Thus, our results indicate that despite most of the research on Tcf7l1 and Wnt/β-catenin signaling being focused on self-renewing ESCs, Tcf7l1 is needed to function as an intrinsic inhibitor of self-renewal during the transition to a primed state. This conclusion provides an explanation for variability in assays measuring differentiation defects of *Tcf7l1* mutant ESCs; since primary defects occur early, measuring lineage marker expression examines the result of secondary or tertiary events that are likely to be influenced by the context of the differentiation assay.

Interestingly, our results help explain seemingly contradictory results concerning the effects of Wnt/β-catenin signaling on pluripotent cells. Both self-renewal and mesoderm specification responses to Wnt/β-catenin have been described previously. Several studies have shown that Wnt/β-catenin signaling promotes or is required for the self-renewal of mouse ESCs (ten Berge et al., 2011; Hao et al., 2006; Ogawa et al., 2006; Sato et al., 2004; Ying et al., 2008). Although some controversy remains from contradictory reports of the effects of Wnts on human ESCs (Dravid et al., 2005; Sato et al., 2004), recent studies show that Wnt/β-catenin stimulates mesoderm differentiation of human ESCs (Davidson et al., 2012; Singh et al., 2012), and the requirement for Wnt/β-catenin signaling in mesoderm specification in mouse embryos has been demonstrated genetically (Huelsken et al., 2000; Kelly et al., 2004; Liu et al., 1999). We recapitulated these distinct responses to Wnt/β-catenin in a cell-based assay in which ESCs were subjected to EpiSC culture conditions. Cells required 2 days to convert from a self-renewal response to a mesoderm specification response to Wnt/β-catenin signaling. The timing of the switch corresponds to that of a previously described switch in cell state detected via the surface protein expression identities of ESCs and EpiSCs (Rugg-Gunn et al., 2012). Thus, Wnt/β-catenin stimulates the self-renewal of naïve cells by preventing the Tcf7l1-mediated transition to a primed state (Fig. 7). Once pluripotent cells reach the primed state, Wnt/β-catenin stimulates differentiation (Fig. 7).

Acknowledgements
We thank members of the B.J.M. laboratory for their thoughtful comments and critical reading of the manuscript and Drs Stephen Duncan, Ian Chambers and Tristan Rodriguez for kind gifts of reagents.

Funding
The work was funded by grants from the American Cancer Society [RSG GGC 112994] and the National Institutes of Health [R01-CA128571] to B.J.M.; and an American Heart Association fellowship to J.A.H. [0610068Z]. Deposited in PMC for release after 12 months.

Competing interests statement
The authors declare no competing financial interests.

Author contributions
J.A.H. and C.IW. performed all experiments. J.A.H. and B.J.M. conceptually designed experiments, analyzed data and wrote the manuscript. B.J.M. supervised the project.

Supplementary material
Supplementary material available online at
http://dev.biologists.org/lookup/suppl/doi:10.1242/dev.087387/-/DC1

References

Acampora, D., Di Giovannantonio, L. G. and Simeone, A. (2013). Otx2 is an intrinsic determinant of the embryonic stem cell state and is required for transition to a stable epiblast stem cell condition. *Development* **140**, 43-55.

Acloque, H., Ocaña, O. H., Matheu, A., Rizzoti, K., Wise, C., Lovell-Badge, R. and Nieto, M. A. (2011). Reciprocal repression between Sox3 and snail transcription factors defines embryonic territories at gastrulation. *Dev. Cell* **21**, 546-558.

Arnold, S. J., Stappert, J., Bauer, A., Kispert, A., Herrmann, B. G. and Kemler, R. (2000). Brachyury is a target gene of the Wnt/beta-catenin signaling pathway. *Mech. Dev.* **91**, 249-258.

Avilion, A. A., Nicolis, S. K., Pevny, L. H., Perez, L., Vivian, N. and Lovell-Badge, R. (2003). Multipotent cell lineages in early mouse development depend on SOX2 function. *Genes Dev.* **17**, 126-140.

Bernemann, C., Greber, B., Ko, K., Sterneckert, J., Han, D. W., Araúzo-Bravo, M. J. and Schöler, H. R. (2011). Distinct developmental ground states of epiblast stem cell lines determine different pluripotency features. *Stem Cells* **29**, 1496-1503.

Boyer, L. A., Lee, T. I., Cole, M. F., Johnstone, S. E., Levine, S. S., Zucker, J. P., Guenther, M. G., Kumar, R. M., Murray, H. L., Jenner, R. G. et al. (2005). Core transcriptional regulatory circuitry in human embryonic stem cells. *Cell* **122**, 947-956.

Brons, I. G., Smithers, L. E., Trotter, M. W., Rugg-Gunn, P., Sun, B., Chuva de Sousa Lopes, S. M., Howlett, S. K., Clarkson, A., Ahrlund-Richter, L., Pedersen, R. A. et al. (2007). Derivation of pluripotent epiblast stem cells from mammalian embryos. *Nature* **448**, 191-195.

Chambers, I. and Tomlinson, S. R. (2009). The transcriptional foundation of pluripotency. *Development* **136**, 2311-2322.
Chambers, I., Colby, D., Robertson, M., Nichols, J., Lee, S., Tweedie, S. and Smith, A. (2003). Functional expression cloning of Nanog, a pluripotency sustaining factor in embryonic stem cells. *Cell* **113**, 643-655.
Cole, M. F., Johnstone, S. E., Newman, J. J., Kagey, M. H. and Young, R. A. (2008). Tcf3 is an integral component of the core regulatory circuitry of embryonic stem cells. *Genes Dev.* **22**, 746-755.
Conlon, F. L., Lyons, K. M., Takaesu, N., Barth, K. S., Kispert, A., Herrmann, B. and Robertson, E. J. (1994). A primary requirement for nodal in the formation and maintenance of the primitive streak in the mouse. *Development* **120**, 1919-1928.
Crompton, L. A., Du Roure, C. and Rodriguez, T. A. (2007). Early embryonic expression patterns of the mouse Flamingo and Prickle orthologues. *Dev. Dyn.* **236**, 3137-3143.
Davidson, K. C., Adams, A. M., Goodson, J. M., McDonald, C. E., Potter, J. C., Berndt, J. D., Biechele, T. L., Taylor, R. J. and Moon, R. T. (2012). Wnt/β-catenin signaling promotes differentiation, not self-renewal, of human embryonic stem cells and is repressed by Oct4. *Proc. Natl. Acad. Sci. USA* **109**, 4485-4490.
Downs, K. M. and Davies, T. (1993). Staging of gastrulating mouse embryos by morphological landmarks in the dissecting microscope. *Development* **118**, 1255-1266.
Dravid, G., Ye, Z., Hammond, H., Chen, G., Pyle, A., Donovan, P., Yu, X. and Cheng, L. (2005). Defining the role of Wnt/beta-catenin signaling in the survival, proliferation, and self-renewal of human embryonic stem cells. *Stem Cells* **23**, 1489-1501.
Evans, M. J. and Kaufman, M. H. (1981). Establishment in culture of pluripotential cells from mouse embryos. *Nature* **292**, 154-156.
Galceran, J., Hsu, S. C. and Grosschedl, R. (2001). Rescue of a Wnt mutation by an activated form of LEF-1: regulation of maintenance but not initiation of Brachyury expression. *Proc. Natl. Acad. Sci. USA* **98**, 8668-8673.
Greber, B., Wu, G., Bernemann, C., Joo, J. Y., Han, D. W., Ko, K., Tapia, N., Sabour, D., Sterneckert, J., Tesar, P. et al. (2010). Conserved and divergent roles of FGF signaling in mouse epiblast stem cells and human embryonic stem cells. *Cell Stem Cell* **6**, 215-226.
Guo, G. and Smith, A. (2010). A genome-wide screen in EpiSCs identifies Nr5a nuclear receptors as potent inducers of ground state pluripotency. *Development* **137**, 3185-3192.
Guo, G., Yang, J., Nichols, J., Hall, J. S., Eyres, I., Mansfield, W. and Smith, A. (2009). Klf4 reverts developmentally programmed restriction of ground state pluripotency. *Development* **136**, 1063-1069.
Guo, G., Huang, Y., Humphreys, P., Wang, X. and Smith, A. (2011). A PiggyBac-based recessive screening method to identify pluripotency regulators. *PLoS ONE* **6**, e18189.
Han, D. W., Tapia, N., Joo, J. Y., Greber, B., Araúzo-Bravo, M. J., Bernemann, C., Ko, K., Wu, G., Stehling, M., Do, J. T. et al. (2010). Epiblast stem cell subpopulations represent mouse embryos of distinct pregastrulation stages. *Cell* **143**, 617-627.
Hao, J., Li, T. G., Qi, X., Zhao, D. F. and Zhao, G. Q. (2006). WNT/beta-catenin pathway up-regulates Stat3 and converges on LIF to prevent differentiation of mouse embryonic stem cells. *Dev. Biol.* **290**, 81-91.
Hart, A. H., Hartley, L., Ibrahim, M. and Robb, L. (2004). Identification, cloning and expression analysis of the pluripotency promoting Nanog genes in mouse and human. *Dev. Dyn.* **230**, 187-198.
Huelsken, J., Vogel, R., Brinkmann, V., Erdmann, B., Birchmeier, C. and Birchmeier, W. (2000). Requirement for beta-catenin in anterior-posterior axis formation in mice. *J. Cell Biol.* **148**, 567-578.
Kelly, O. G., Pinson, K. I. and Skarnes, W. C. (2004). The Wnt co-receptors Lrp5 and Lrp6 are essential for gastrulation in mice. *Development* **131**, 2803-2815.
Kim, J., Chu, J., Shen, X., Wang, J. and Orkin, S. H. (2008). An extended transcriptional network for pluripotency of embryonic stem cells. *Cell* **132**, 1049-1061.
Lawson, K. A., Meneses, J. J. and Pedersen, R. A. (1991). Clonal analysis of epiblast fate during germ layer formation in the mouse embryo. *Development* **113**, 891-911.
Liang, J., Wan, M., Zhang, Y., Gu, P., Xin, H., Jung, S. Y., Qin, J., Wong, J., Cooney, A. J., Liu, D. et al. (2008). Nanog and Oct4 associate with unique transcriptional repression complexes in embryonic stem cells. *Nat. Cell Biol.* **10**, 731-739.
Liu, P., Wakamiya, M., Shea, M. J., Albrecht, U., Behringer, R. R. and Bradley, A. (1999). Requirement for Wnt3 in vertebrate axis formation. *Nat. Genet.* **22**, 361-365.
Loh, Y. H., Wu, Q., Chew, J. L., Vega, V. B., Zhang, W., Chen, X., Bourque, G., George, J., Leong, B., Liu, J. et al. (2006). The Oct4 and Nanog transcription network regulates pluripotency in mouse embryonic stem cells. *Nat. Genet.* **38**, 431-440.
Marson, A., Levine, S. S., Cole, M. F., Frampton, G. M., Brambrink, T., Johnstone, S., Guenther, M. G., Johnston, W. K., Wernig, M., Newman, J. et al. (2008). Connecting microRNA genes to the core transcriptional regulatory circuitry of embryonic stem cells. *Cell* **134**, 521-533.
Martello, G., Sugimoto, T., Diamanti, E., Joshi, A., Hannah, R., Ohtsuka, S., Göttgens, B., Niwa, H. and Smith, A. (2012). Esrrb is a pivotal target of the Gsk3/Tcf3 axis regulating embryonic stem cell self-renewal. *Cell Stem Cell* **11**, 491-504.
Martin, G. R. (1981). Isolation of a pluripotent cell line from early mouse embryos cultured in medium conditioned by teratocarcinoma stem cells. *Proc. Natl. Acad. Sci. USA* **78**, 7634-7638.
Merrill, B. J., Pasolli, H. A., Polak, L., Rendl, M., García-García, M. J., Anderson, K. V. and Fuchs, E. (2004). Tcf3: a transcriptional regulator of axis induction in the early embryo. *Development* **131**, 263-274.
Misra, R. P., Bronson, S. K., Xiao, Q., Garrison, W., Li, J., Zhao, R. and Duncan, S. A. (2001). Generation of single-copy transgenic mouse embryos directly from ES cells by tetraploid embryo complementation. *BMC Biotechnol.* **1**, 12.
Mitsui, K., Tokuzawa, Y., Itoh, H., Segawa, K., Murakami, M., Takahashi, K., Maruyama, M., Maeda, M. and Yamanaka, S. (2003). The homeoprotein Nanog is required for maintenance of pluripotency in mouse epiblast and ES cells. *Cell* **113**, 631-642.
Morkel, M., Huelsken, J., Wakamiya, M., Ding, J., van de Wetering, M., Clevers, H., Taketo, M. M., Behringer, R. R., Shen, M. M. and Birchmeier, W. (2003). Beta-catenin regulates Cripto- and Wnt3-dependent gene expression programs in mouse axis and mesoderm formation. *Development* **130**, 6283-6294.
Nichols, J., Zevnik, B., Anastassiadis, K., Niwa, H., Klewe-Nebenius, D., Chambers, I., Schöler, H. and Smith, A. (1998). Formation of pluripotent stem cells in the mammalian embryo depends on the POU transcription factor Oct4. *Cell* **95**, 379-391.
Niwa, H., Miyazaki, J. and Smith, A. G. (2000). Quantitative expression of Oct-3/4 defines differentiation, dedifferentiation or self-renewal of ES cells. *Nat. Genet.* **24**, 372-376.
Ogawa, K., Nishinakamura, R., Iwamatsu, Y., Shimosato, D. and Niwa, H. (2006). Synergistic action of Wnt and LIF in maintaining pluripotency of mouse ES cells. *Biochem. Biophys. Res. Commun.* **343**, 159-166.
Osorno, R., Tsakiridis, A., Wong, F., Cambray, N., Economou, C., Wilkie, R., Blin, G., Scotting, P. J., Chambers, I. and Wilson, V. (2012). The developmental dismantling of pluripotency is reversed by ectopic Oct4 expression. *Development* **139**, 2288-2298.
Pereira, L., Yi, F. and Merrill, B. J. (2006). Repression of Nanog gene transcription by Tcf3 limits embryonic stem cell self-renewal. *Mol. Cell. Biol.* **26**, 7479-7491.
Renfree, M. B. and Shaw, G. (2000). Diapause. *Annu. Rev. Physiol.* **62**, 353-375.
Rivera-Pérez, J. A., Jones, V. and Tam, P. P. (2010). Culture of whole mouse embryos at early postimplantation to organogenesis stages: developmental staging and methods. *Methods Enzymol.* **476**, 185-203.
Rugg-Gunn, P. J., Cox, B. J., Lanner, F., Sharma, P., Ignatchenko, V., McDonald, A. C., Garner, J., Gramolini, A. O., Rossant, J. and Kislinger, T. (2012). Cell-surface proteomics identifies lineage-specific markers of embryo-derived stem cells. *Dev. Cell* **22**, 887-901.
Salomonis, N., Schlieve, C. R., Pereira, L., Wahlquist, C., Colas, A., Zambon, A. C., Vranizan, K., Spindler, M. J., Pico, A. R., Cline, M. S. et al. (2010). Alternative splicing regulates mouse embryonic stem cell pluripotency and differentiation. *Proc. Natl. Acad. Sci. USA* **107**, 10514-10519.
Sato, N., Meijer, L., Skaltsounis, L., Greengard, P. and Brivanlou, A. H. (2004). Maintenance of pluripotency in human and mouse embryonic stem cells through activation of Wnt signaling by a pharmacological GSK-3-specific inhibitor. *Nat. Med.* **10**, 55-63.
Shih, Y. H., Kuo, C. L., Hirst, C. S., Dee, C. T., Liu, Y. R., Laghari, Z. A. and Scotting, P. J. (2010). SoxB1 transcription factors restrict organizer gene expression by repressing multiple events downstream of Wnt signalling. *Development* **137**, 2671-2681.
Singh, A. M., Reynolds, D., Cliff, T., Ohtsuka, S., Mattheyses, A. L., Sun, Y., Menendez, L., Kulik, M. and Dalton, S. (2012). Signaling network crosstalk in human pluripotent cells: a Smad2/3-regulated switch that controls the balance between self-renewal and differentiation. *Cell Stem Cell* **10**, 312-326.
Snow, M. H. L. (1977). Gastrulation in the mouse: growth and regionalization of the epiblast. *J. Embryol. Exp. Morphol.* **42**, 293-303.
Tam, P. P., Parameswaran, M., Kinder, S. J. and Weinberger, R. P. (1997). The allocation of epiblast cells to the embryonic heart and other mesodermal lineages: the role of ingression and tissue movement during gastrulation. *Development* **124**, 1631-1642.
Tam, W. L., Lim, C. Y., Han, J., Zhang, J., Ang, Y. S., Ng, H. H., Yang, H. and Lim, B. (2008). T-cell factor 3 regulates embryonic stem cell pluripotency and self-renewal by the transcriptional control of multiple lineage pathways. *Stem Cells* **26**, 2019-2031.
ten Berge, D., Kurek, D., Blauwkamp, T., Koole, W., Maas, A., Eroglu, E., Siu, R. K. and Nusse, R. (2011). Embryonic stem cells require Wnt proteins to prevent differentiation to epiblast stem cells. *Nat. Cell Biol.* **13**, 1070-1075.

Tesar, P. J., Chenoweth, J. G., Brook, F. A., Davies, T. J., Evans, E. P., Mack, D. L., Gardner, R. L. and McKay, R. D. (2007). New cell lines from mouse epiblast share defining features with human embryonic stem cells. *Nature* **448**, 196-199.

Thomson, M., Liu, S. J., Zou, L. N., Smith, Z., Meissner, A. and Ramanathan, S. (2011). Pluripotency factors in embryonic stem cells regulate differentiation into germ layers. *Cell* **145**, 875-889.

Voiculescu, O., Bertocchini, F., Wolpert, L., Keller, R. E. and Stern, C. D. (2007). The amniote primitive streak is defined by epithelial cell intercalation before gastrulation. *Nature* **449**, 1049-1052.

Wang, J., Rao, S., Chu, J., Shen, X., Levasseur, D. N., Theunissen, T. W. and Orkin, S. H. (2006). A protein interaction network for pluripotency of embryonic stem cells. *Nature* **444**, 364-368.

Wang, Z., Oron, E., Nelson, B., Razis, S. and Ivanova, N. (2012). Distinct lineage specification roles for NANOG, OCT4, and SOX2 in human embryonic stem cells. *Cell Stem Cell* **10**, 440-454.

Wilkinson, D. G., Bhatt, S. and Herrmann, B. G. (1990). Expression pattern of the mouse T gene and its role in mesoderm formation. *Nature* **343**, 657-659.

Wray, J., Kalkan, T., Gomez-Lopez, S., Eckardt, D., Cook, A., Kemler, R. and Smith, A. (2011). Inhibition of glycogen synthase kinase-3 alleviates Tcf3 repression of the pluripotency network and increases embryonic stem cell resistance to differentiation. *Nat. Cell Biol.* **13**, 838-845.

Wu, C. I., Hoffman, J. A., Shy, B. R., Ford, E. M., Fuchs, E., Nguyen, H. and Merrill, B. J. (2012). Function of Wnt/β-catenin in counteracting Tcf3 repression through the Tcf3-β-catenin interaction. *Development* **139**, 2118-2129.

Yamaguchi, S., Kimura, H., Tada, M., Nakatsuji, N. and Tada, T. (2005). Nanog expression in mouse germ cell development. *Gene Expr. Patterns* **5**, 639-646.

Yeom, Y. I., Fuhrmann, G., Ovitt, C. E., Brehm, A., Ohbo, K., Gross, M., Hübner, K. and Schöler, H. R. (1996). Germline regulatory element of Oct-4 specific for the totipotent cycle of embryonal cells. *Development* **122**, 881-894.

Yi, F., Pereira, L. and Merrill, B. J. (2008). Tcf3 functions as a steady state limiter of transcriptional programs of mouse embryonic stem cell self renewal. *Stem Cells* **26**, 1951-1960.

Yi, F., Pereira, L., Hoffman, J. A., Shy, B. R., Yuen, C. M., Liu, D. R. and Merrill, B. J. (2011). Opposing effects of Tcf3 and Tcf1 control Wnt stimulation of embryonic stem cell self-renewal. *Nat. Cell Biol.* **13**, 762-770.

Ying, Q. L., Wray, J., Nichols, J., Batlle-Morera, L., Doble, B., Woodgett, J., Cohen, P. and Smith, A. (2008). The ground state of embryonic stem cell self-renewal. *Nature* **453**, 519-523.

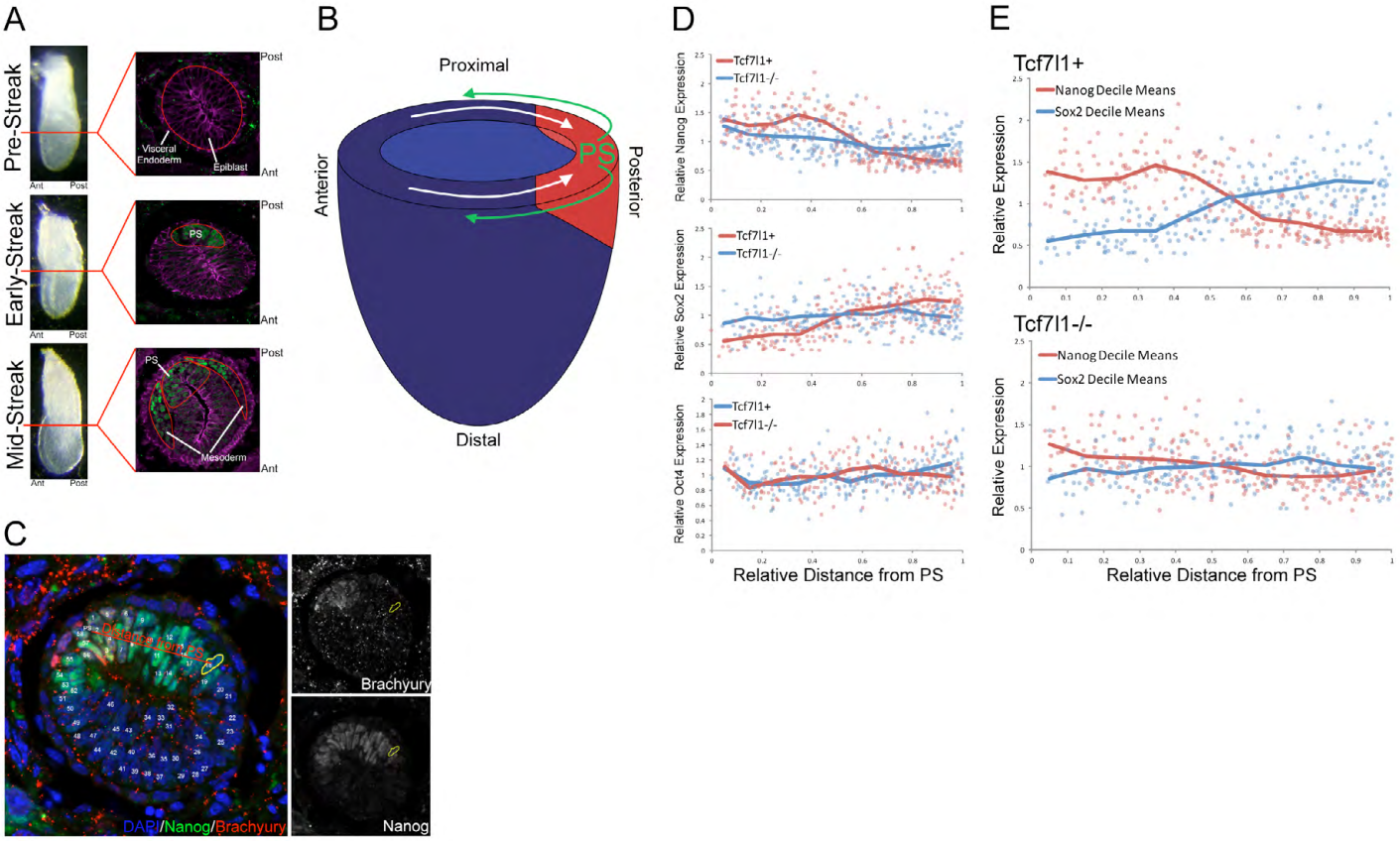

Fig. S1. Schematic of embryo staging, sectioning, cell movements and quantification of immunofluorescent staining. See also Figs 1 and 2. (**A**) Intact gastrulation stage embryos (left) were sectioned within their decidua along a transverse axis, illustrated with the red line, to generate an embryo section (right). Sections of embryos (right) are shown in the same orientation as in Fig. 1. These three images are identical to those in Fig. 1B-B″. Epiblast and visceral endoderm cells express membrane-associated E-cadherin (magenta) throughout gastrulation. Pre-streak embryos have an internal embryonic ectoderm layer (epiblast; enclosed by red oval) surrounded by the thin visceral endoderm, but do not have mesoderm forming at the PS. Early-streak embryos display a nascent PS structure (enclosed by red line) at the posterior, and activation of mesoderm gene expression (green). Mid-streak embryos have a PS structure, and mesoderm cells migrating laterally from the PS (red 'wings') lacking E-cadherin. Ant, anterior; post, posterior; PS, primitive streak. (**B**) Diagram of cell movements in the early streak epiblast summarized from several studies (Lawson et al., 1991; Tam et al., 1997). Movement of epiblast cells is depicted with white arrows, and movement of mesoderm cells is depicted with green arrows. During PS formation, cells in the proximal epiblast move from the anterior towards the posterior and enter into the PS where they specify mesoderm, exit the epiblast and form a new layer of mesoderm cells that migrate laterally towards the anterior. Cells in the distal anterior epiblast move proximally to replace the cells moving towards the posterior. (**C**) Example of an embryo used for quantification of immunofluorescent staining. Each nucleus in the epiblast was numbered and the middle of the PS was marked. The straight line distance from the PS to the center of each nucleus was measured. Each nucleus was then outlined and the mean intensity of signal in each RGB channel was determined. Nucleus 18 is outlined in yellow as an example measuring Nanog and brachyury nuclear intensities. (**D**) Overlay of immunofluorescent quantification from *Tcf7l1*$^{+}$ (red) and *Tcf7l1*$^{-/-}$ (blue) embryos depicted in Figs 1 and 2 for Nanog (top), Sox2 (middle) and Oct4 (bottom). Lines represent mean immunofluorescence intensities for nuclei grouped into ten deciles by distance from PS. (**E**) Overlay of immunofluorescence quantification of Nanog and Sox2 expression from *Tcf7l1*$^{+}$ (top) and *Tcf7l1*$^{-/-}$ (bottom) embryos from Figs 1 and 2. Lines represent mean immunofluorescence intensities for nuclei grouped into ten deciles by distance from PS. Note that the reciprocal patterns of Nanog and Sox2 immunofluorescence intensity are greatly reduced in *Tcf7l1*$^{-/-}$ embryos.

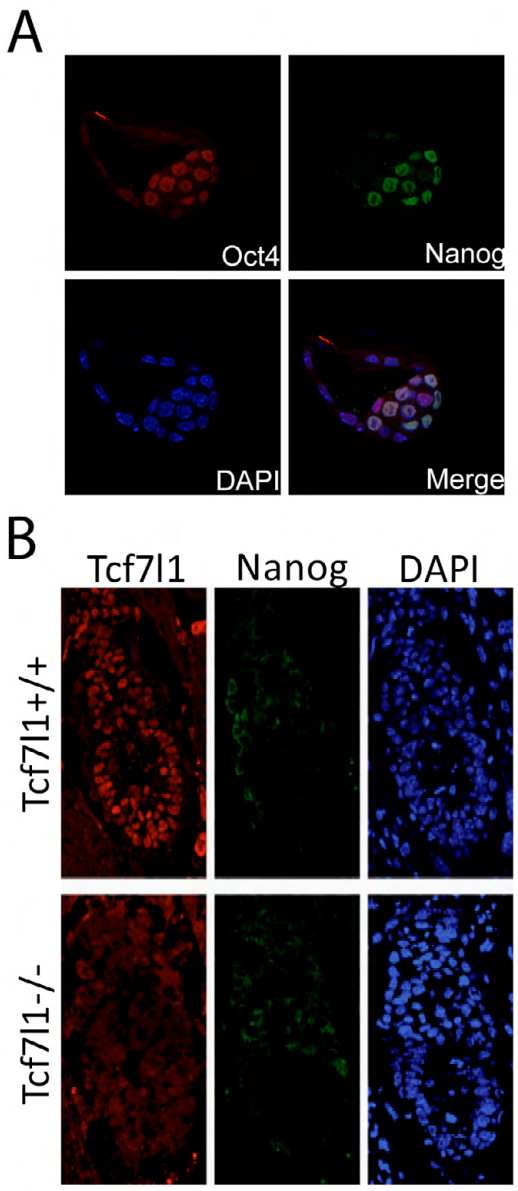

Fig. S2. Nanog and Oct4 expression in blastocysts and E5.5 embryos. (**A**) Confocal microscopy section through a representative of 40 blastocysts obtained from breeding *Tcf7l1*$^{+/-}$ mice. (**B**) Immunofluorescent staining for Tcf7l1 (red), Nanog (green) and nuclei (DAPI, blue) on sagittal sections of *Tcf7l1*$^{+}$ (top) and *Tcf7l1*$^{-/-}$ (bottom) embryos at E5.5.

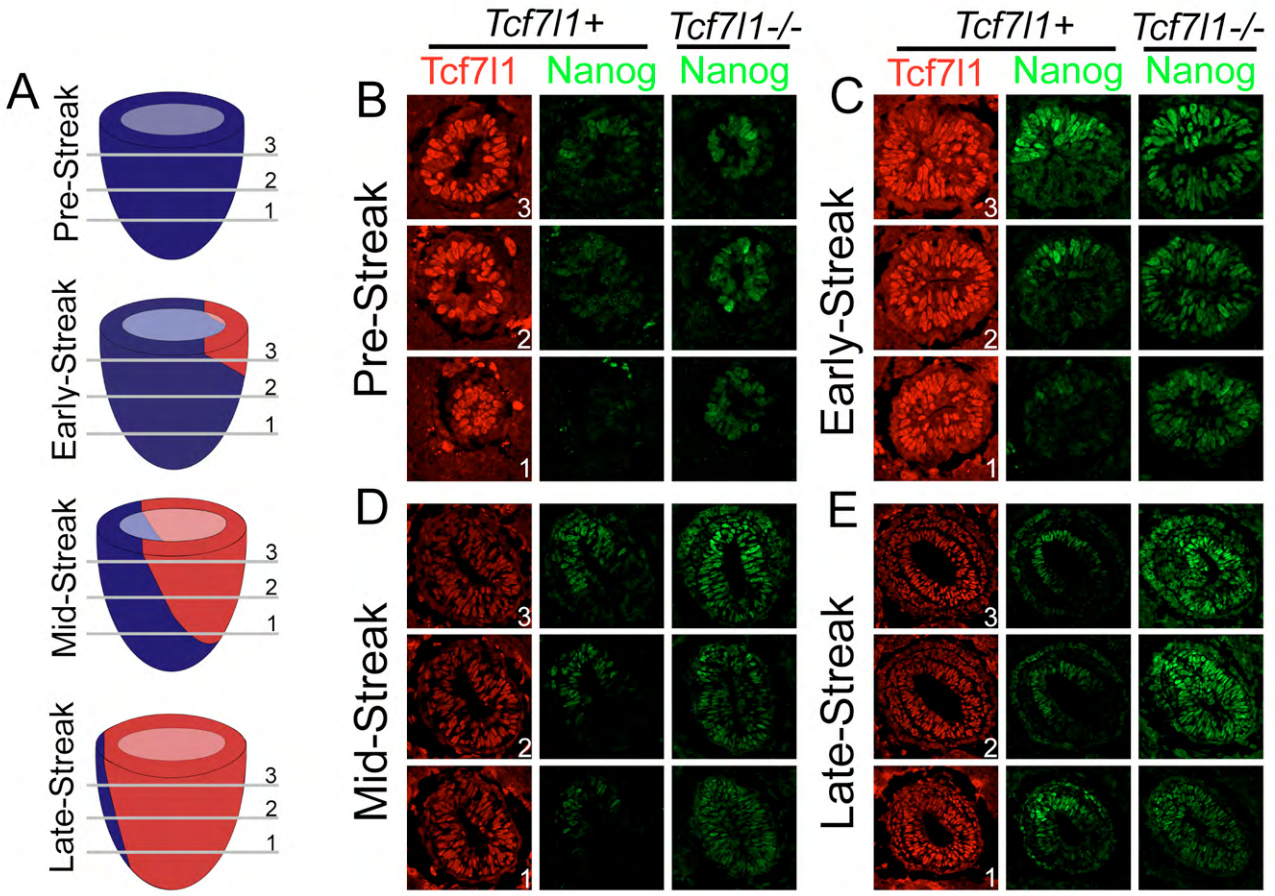

Fig. S3. Three-dimensional analysis of Nanog expression during PS formation. (**A**) In the schematic of experimental design (left), blue represents the epiblast and red represents the area covered by the PS and mesoderm. (**B-E**) Tcf7l1 (red) and Nanog (green) protein expression in *Tcf7l1*$^{+}$ and *Tcf7l1*$^{-/-}$ embryos at pre- (B), early- (C), mid- (D) and late- (E) streak stages. Numbers 1-3 correspond to the approximate position in the embryo shown in the schematic.

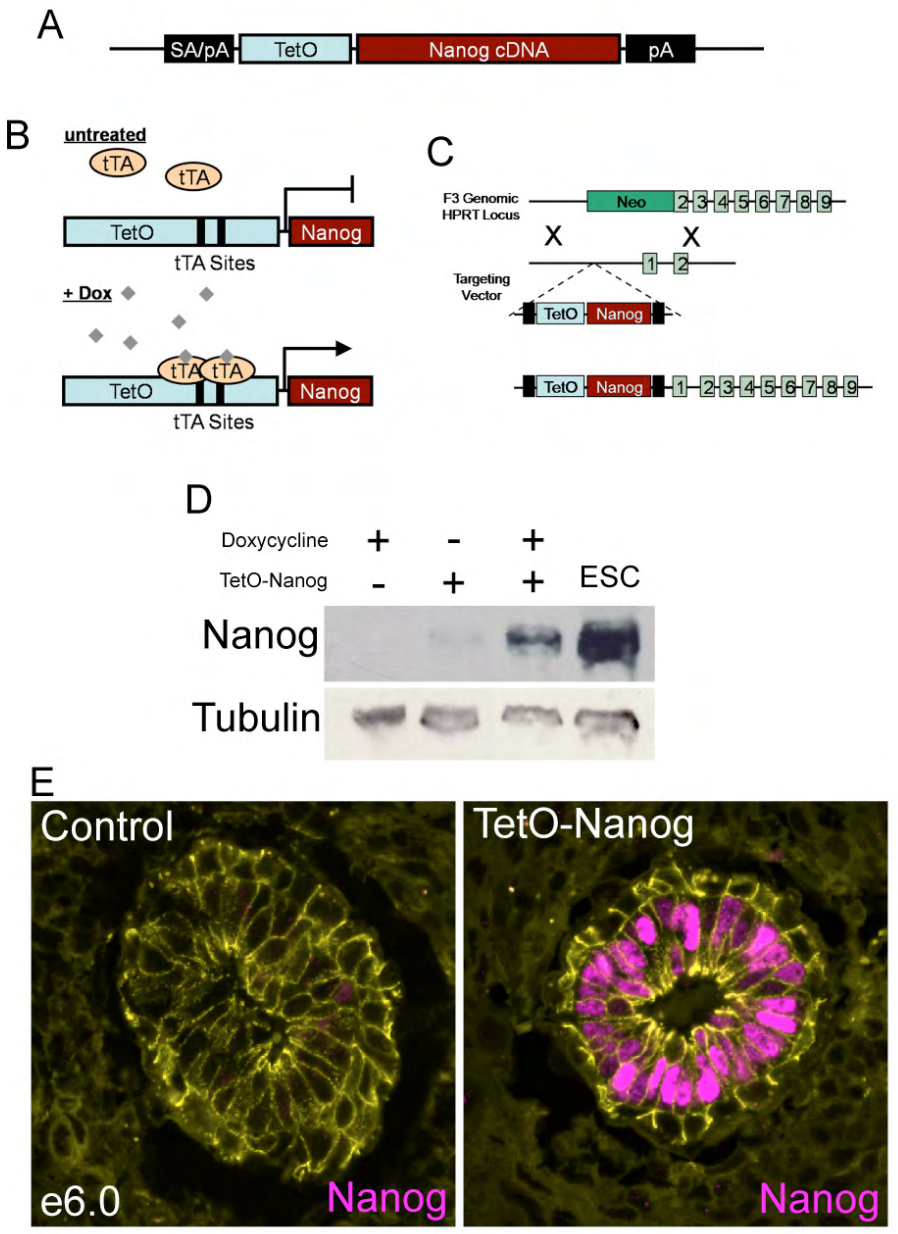

Fig. S4. Doxycycline-inducible *Nanog* transgenic mice. (**A**) Design of the TetO-Nanog gene cassette. Tet operator (TetO) and *Nanog* cDNA flanked by an upstream splice acceptor and polyadenylation signal sequence (SA/PA) and downstream polyadenylation signal sequence (PA). (**B**) Tet-On induction mechanism. In the absence of doxycycline, the Tet transactivator protein (tTA) is unable to bind to tTA target sequences in the TetO and Nanog expression is not induced. In the presence of doxycycline, the tTA protein binds to tTA target sequences in the TetO and promotes transcription of *Nanog* mRNA. (**C**) Genomic integration of the TetO-Nanog gene cassette by homologous recombination removes neomycin resistance and restores HPRT gene function in F3 cells. (**D**) Western blot for Nanog and tubulin in U2OS-tTA cells transfected with the TetO-Nanog targeting vector and treated with doxycycline. Note that Nanog expression was only induced in the presence of both doxycycline and the TetO-Nanog vector. ESC protein was included as a positive control for Nanog expression. (**E**) Immunofluorescent staining for Nanog (magenta) and E-cadherin (yellow) on transverse sections of doxycycline-induced control (left) and TetO-Nanog (right) embryos at E6.0. Note that Nanog is ectopically expressed throughout the epiblast of the TetO-Nanog embryo prior to induction of Nanog expression in the epiblast of the control embryo.

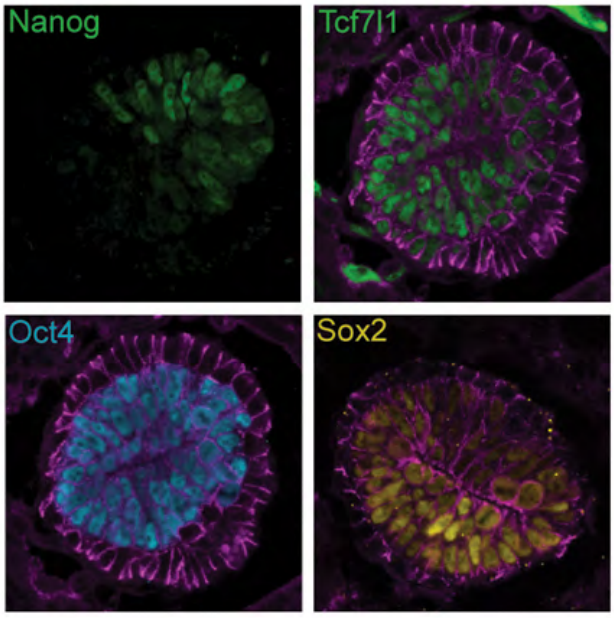

Fig. S5. Pluripotency factor expression in non-overexpressing *Nanog* transgenic controls. Immunofluorescent detection of Nanog, Tcf7l1, Oct4 and Sox2 protein in transverse sections of early-streak stage non-overexpressing *Nanog* transgenic controls. Note that the patterns of Nanog, Tcf7l1, Oct4 and Sox2 expression are indistinguishable from those in *Tcf7l1*$^{+/+}$ embryos (Fig. 1) and Nanog-overexpressing embryos (Fig. 2).

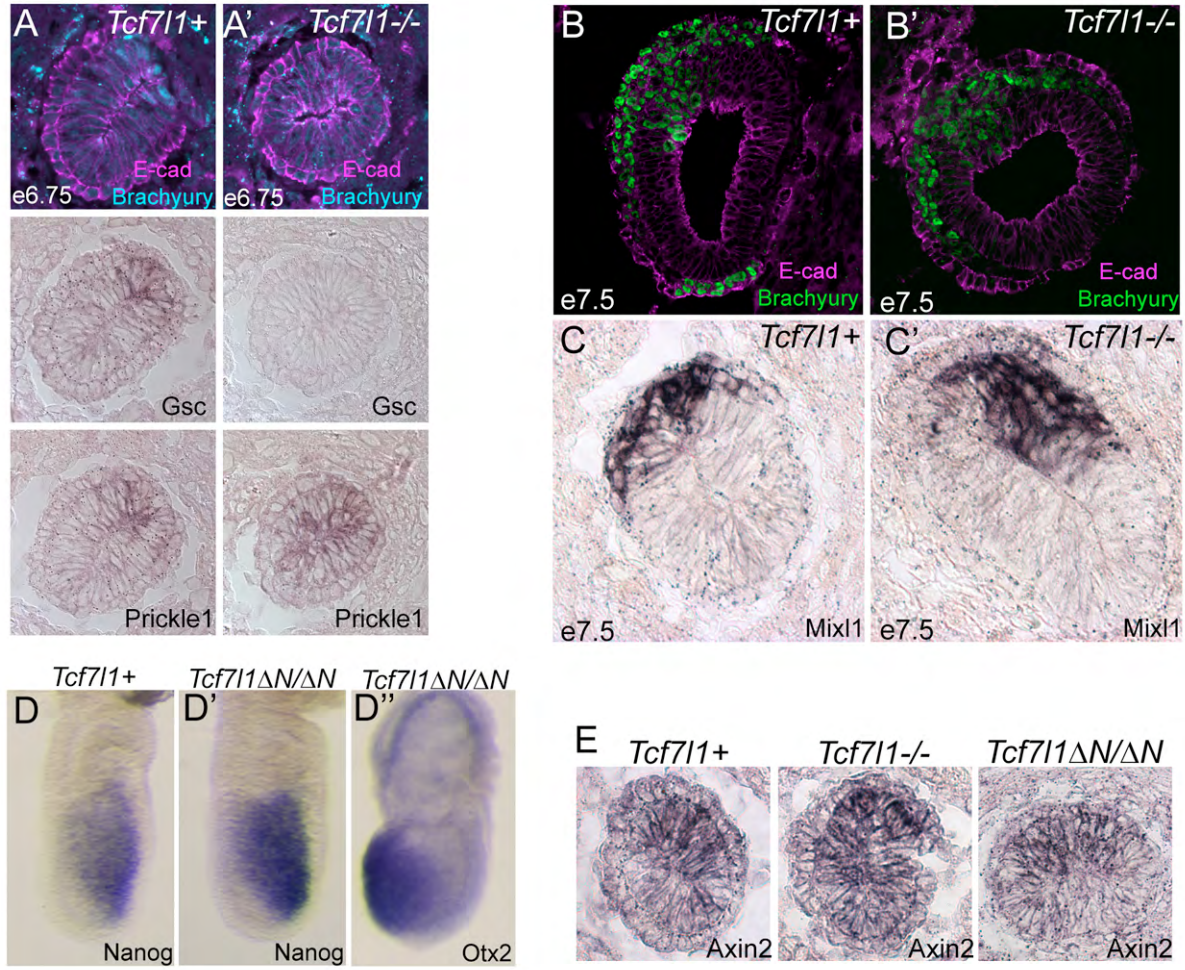

Fig. S6. Mesoderm genes are expressed in *Tcf7l1*$^{-/-}$ embryos after the delay and Tcf7l1/β-catenin interaction is not required for regulation of Nanog expression or Wnt/β-catenin mediated gene expression. (**A**,**A′**) Immunofluorescent detection of brachyury (cyan) and E-cadherin (magenta) and *in situ* hybridization of *Prickle1* and *Gsc* in early-streak *Tcf7l1*$^{+}$ (A) and *Tcf7l1*$^{-/-}$ (A′) embryos. (**B**,**B′**) Brachyury (green) and E-cadherin (magenta) immunofluorescent staining of a transverse section of an E7.5 *Tcf7l1*$^{+}$ (B) or *Tcf7l1*$^{-/-}$ (B′) embryo. Posterior is at the upper left of each image. Note that the anterior domain of brachyury expression detected in the prospective notochord of *Tcf7l1*$^{+}$ embryos is absent in *Tcf7l1*$^{-/-}$ embryos. (**C**,**C′**) *Mixl1* in situ hybridization on a transverse section of E7.5 *Tcf7l1*$^{+}$ (C) or *Tcf7l1*$^{-/-}$ (C′) embryo. Posterior is at the upper left of each image. (**D-D″**) Whole-mount *in situ* hybridization detection of *Nanog* (D,D′) and *Otx2* mRNA (D″) in *Tcf7l1*$^{+}$ and *Tcf7l1*$^{\Delta N/\Delta N}$ embryos. Each image is a lateral view of the embryo with posterior to the right. (**E**) *In situ* hybridization for *Axin2* on transverse sections of early-streak embryos. No reproducible difference was detected between *Tcf7l1*$^{+}$ (left), *Tcf7l1*$^{-/-}$ (middle) and *Tcf7l1*$^{\Delta N/\Delta N}$ (right) embryos. In each image, posterior is at the top.

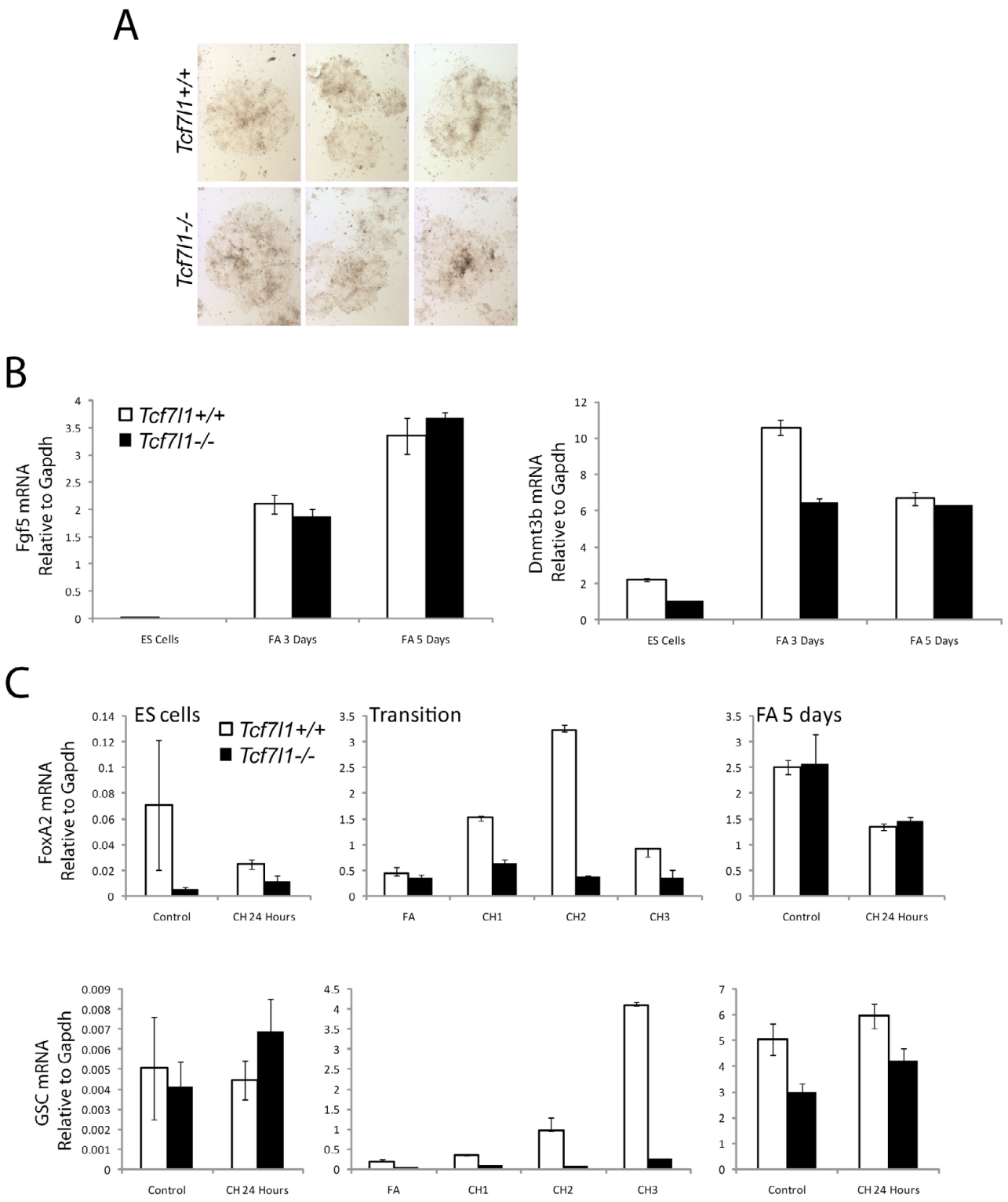

Fig. S7. Tcf7l1 is not required for induction of mesoderm gene expression. (**A**) Representative images of alkaline phosphatase-stained *Tcf7l1*$^{+/+}$ (top) and *Tcf7l1*$^{-/-}$ (bottom) colonies after 5 days in EpiSC culture conditions. Note that both *Tcf7l1*$^{+/+}$ and *Tcf7l1*$^{-/-}$ colonies are AP-negative and exhibit EpiSC-like colony morphology. (**B**) Quantitative RT-PCR assays measuring *Fgf5* and *Dnmt3b* mRNA expression relative to *Gapdh* in untreated ESCs and ESCs after 3 or 5 days in EpiSC conditions. (**C**) Quantitative RT-PCR assays measuring the levels of endoderm genes *Foxa2* (top) and *Gsc* (bottom) in response to CH in ESCs (left), in cells undergoing transition (middle), and in cells after 5 days of culture in EpiSC conditions (right) as in Fig. 6E. Values are normalized to the level of *Gapdh* expression in each sample. White bars represent *Tcf7l1*$^{+/+}$ cells and black bars represent *Tcf7l1*$^{-/-}$ cells.